SUPPLEMENATARY MATERIALS

Next Generation QTAIM for the Design of Emitters Exhibiting Thermally-Activated Delayed Fluorescence (TADF)

Zi Li, Xing Nie, Alireza Azizi, Yong Yang, Tianlv Xu, Steven R. Kirk* and Samantha Jenkins*

Key Laboratory of Chemical Biology and Traditional Chinese Medicine Research and Key Laboratory of Resource National and Local Joint Engineering Laboratory for New Petro-chemical Materials and Fine Utilization of Resources, College of Chemistry and Chemical Engineering, Hunan Normal University, Changsha, Hunan 410081, China

email: steven.kirk@cantab.net
email: samanthajsuman@gmail.com

1. Supplementary Materials S1. The QTAIM $\{q,q'\}$ path-packets of the cyclazine molecular graph for the S_1 and T_1 states without and with an applied electric (**E**)-field.

2. Supplementary Materials S2. The QTAIM $\{p,p'\}$ path-packets of the cyclazine molecular graph for the S_1 and T_1 states without and with an applied electric (**E**)-field.

3. Supplementary Materials S3. The values of the precession $\mathbb{K}$ along the C3-C5 *BCP* bond-paths for the S_1 and T_1 states

1. Supplementary Materials S1.

For the precession of the {$\boldsymbol{q}$,$\boldsymbol{q'}$} path-packet, defined by the $\underline{\mathbf{e}}_2$ eigenvector, about the bond-path, $\beta = (\pi/2 - \alpha)$ and α is defined by equation **(2)** and the right panel of **Scheme 1** of the main text, we can write an expression $\mathbb{K}'$ for the bond-path-flexibility:

$$\mathbb{K}' = 1 - \cos^2\beta, \qquad \text{where } \cos\beta = \underline{\mathbf{e}}_2 \cdot \underline{\mathbf{u}}, \quad \beta = (\pi/2 - \alpha) \quad \text{and} \quad 0 \leq \mathbb{K}' \leq 1 \qquad \textbf{(2)}$$

For $\mathbb{K}' = 0$ we have a maximum degree of facile character and for $\mathbb{K} = 1$ we have the minimum degree of facile character and values of $\mathbb{K}' = 0$ and $\mathbb{K}' = 1$ therefore indicate bond-paths with the lowest and highest tendencies towards bond-path-flexibility respectively.

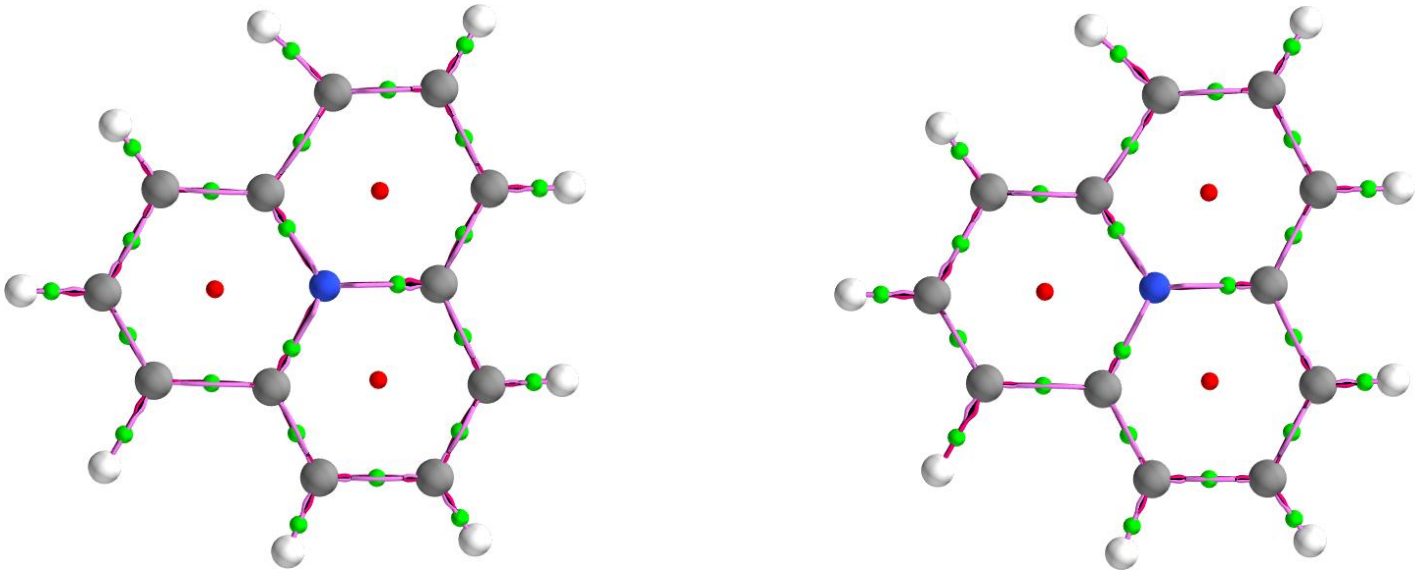

(a)

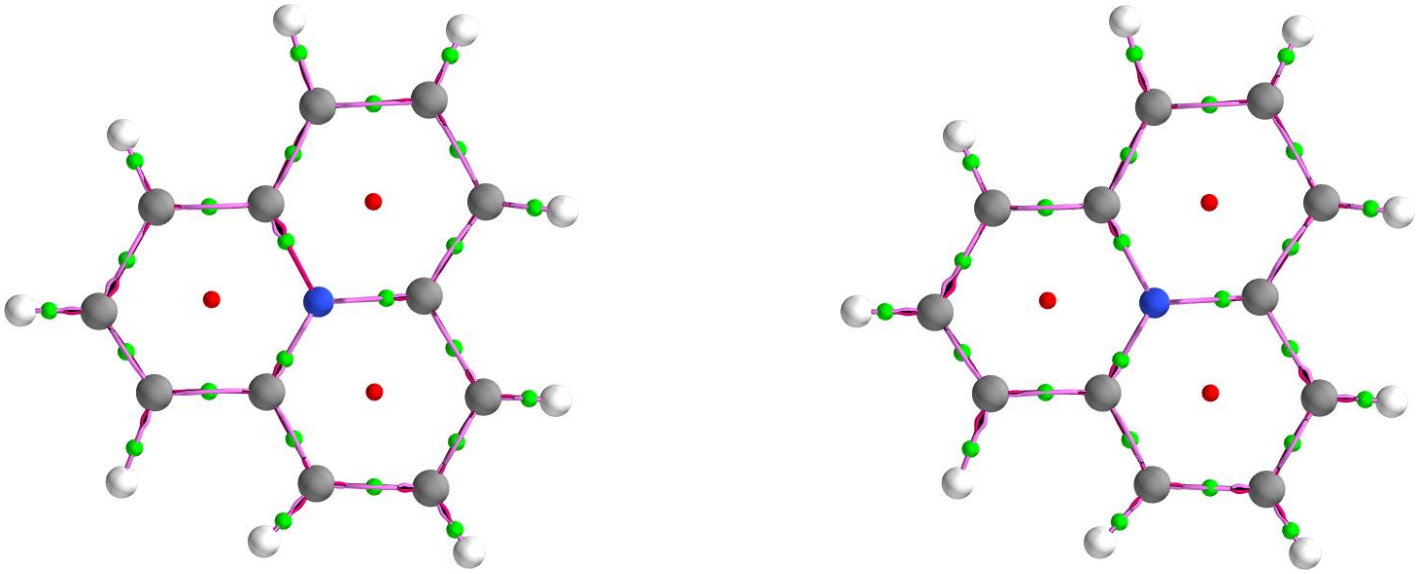

(b)

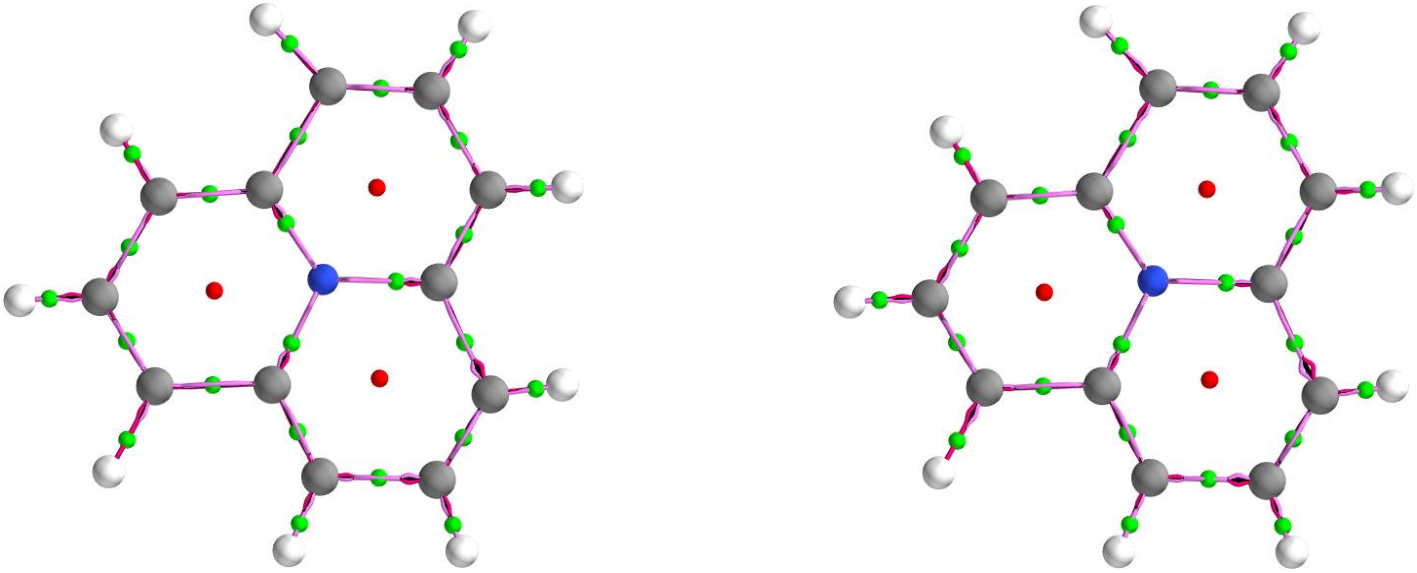

(c)

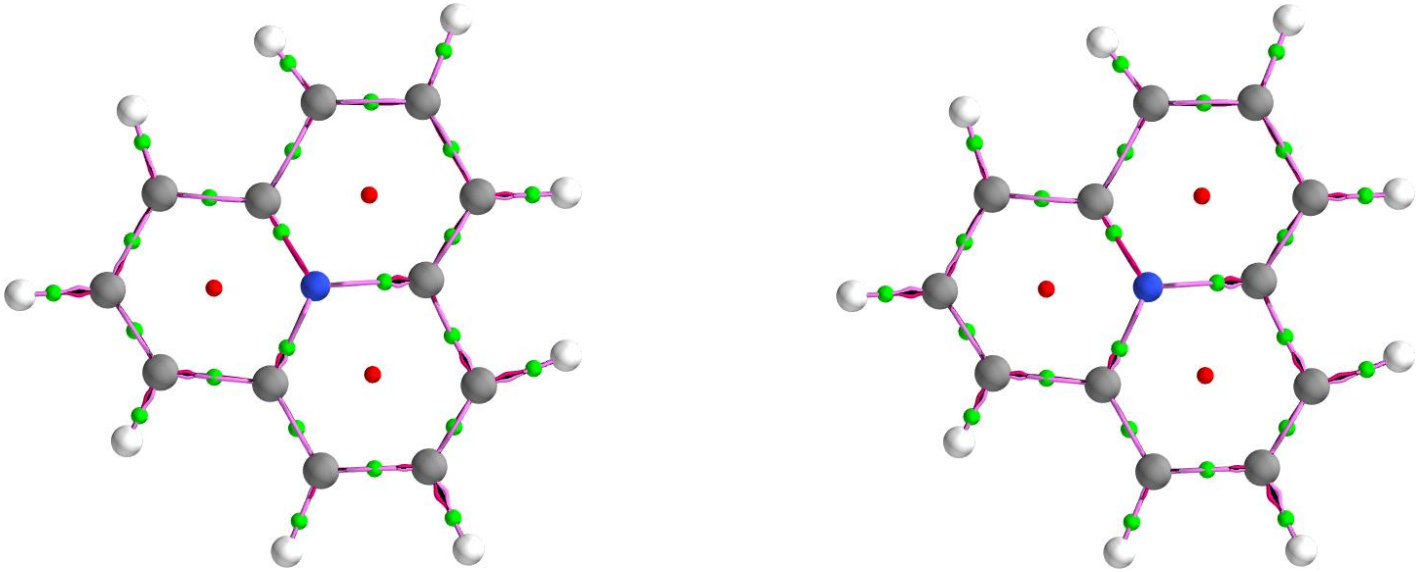

(d)

Figure S1(I). The QTAIM ***{q,q'}*** path-packets of the cyclazine molecular graph corresponding to the S_1 (left panel) and T_1 (right panel) states of the unchirped pulse 30 fs, 40 fs, 50 fs and 75fs with a positive energy gap $\Delta E(S_1\text{-}T_1) > 0$ are presented in each of sub-figures **(a-d)** respectively.

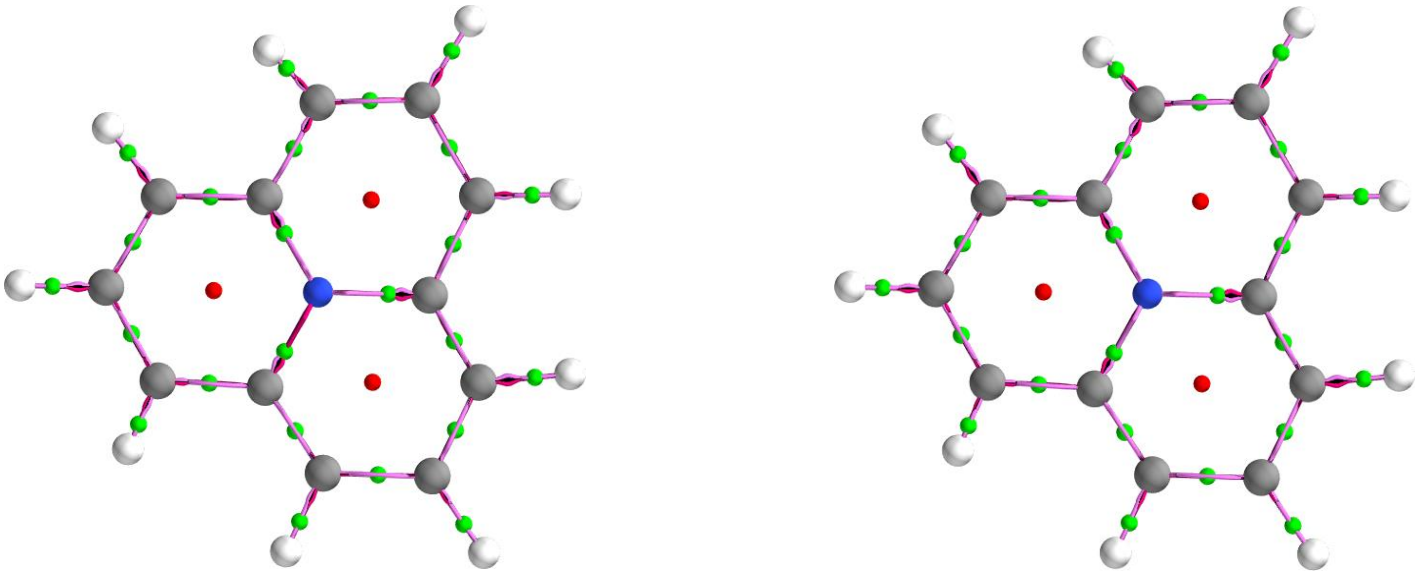

(a)

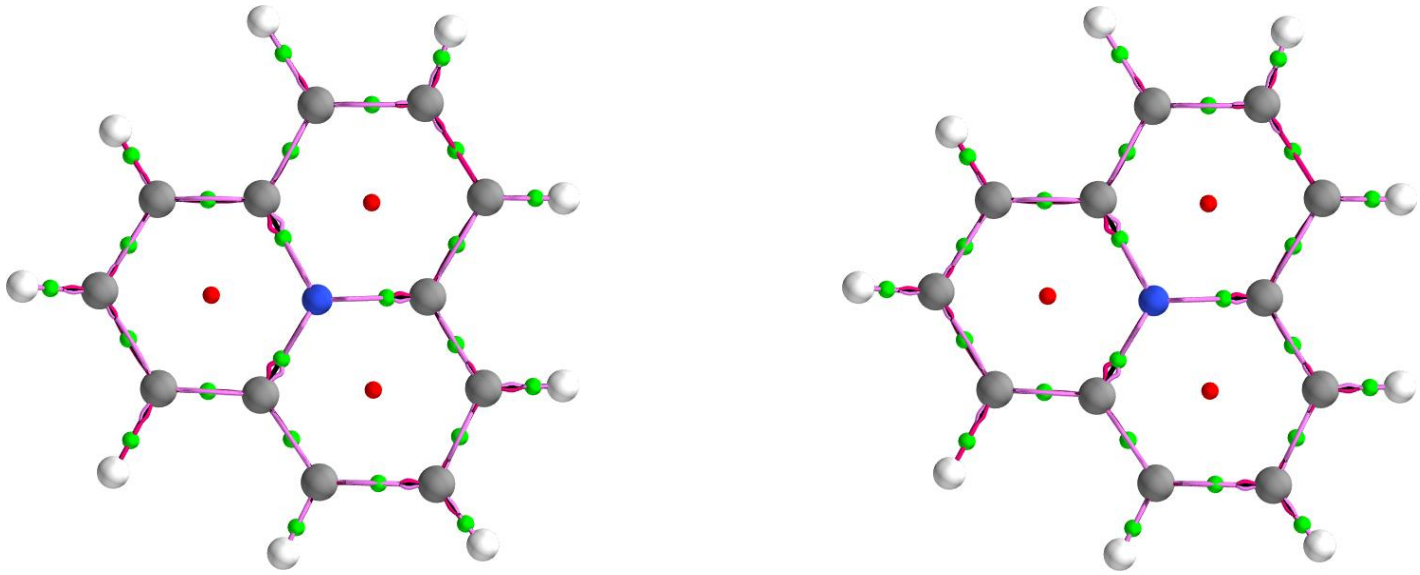

(b)

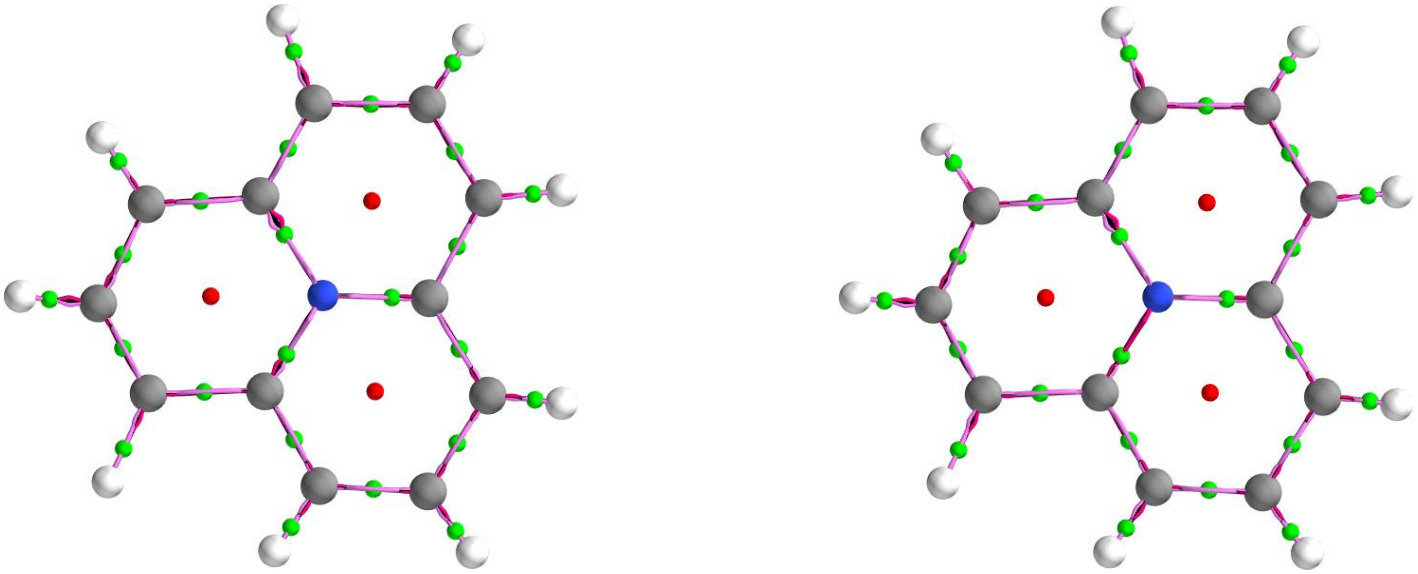

(c)

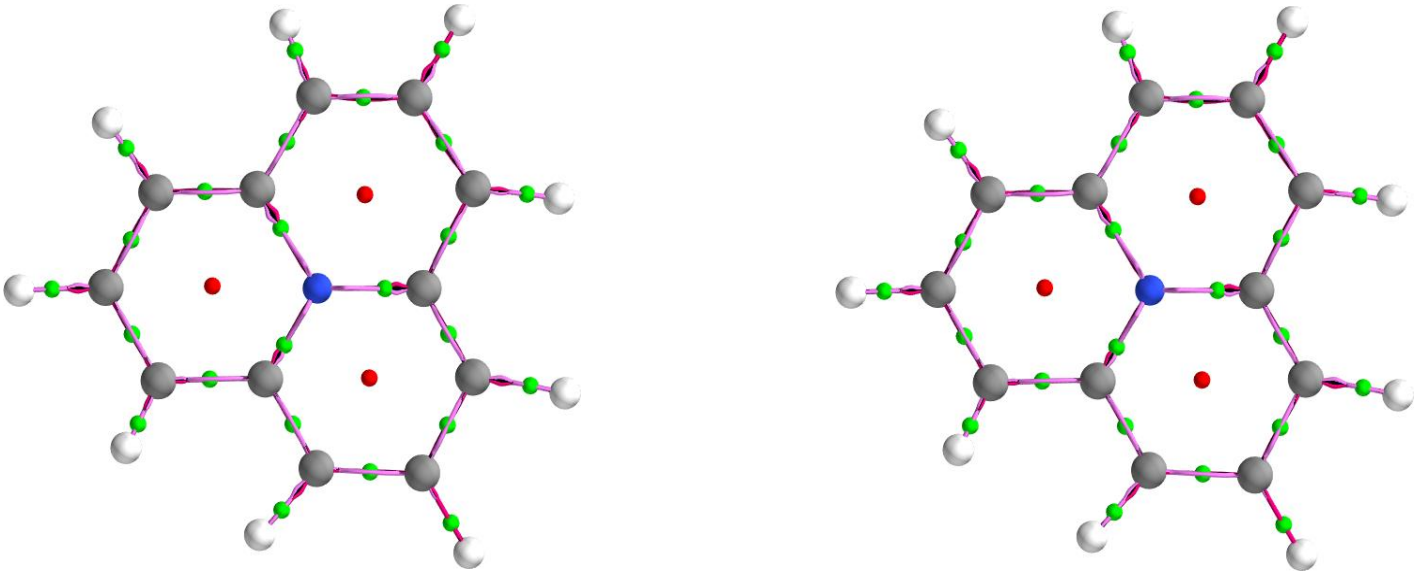

(d)

Figure S1(II). The QTAIM ***{q,q'}*** path-packets of the cyclazine molecular graph corresponding to the S_1 (left panel) and T_1 (right panel) states of the unchirped pulse 5fs, 10fs, 60fs and 65fs with a negative energy gap $\Delta E(S_1\text{-}T_1) < 0$ are presented in each of sub-figures **(a-d)** respectively.

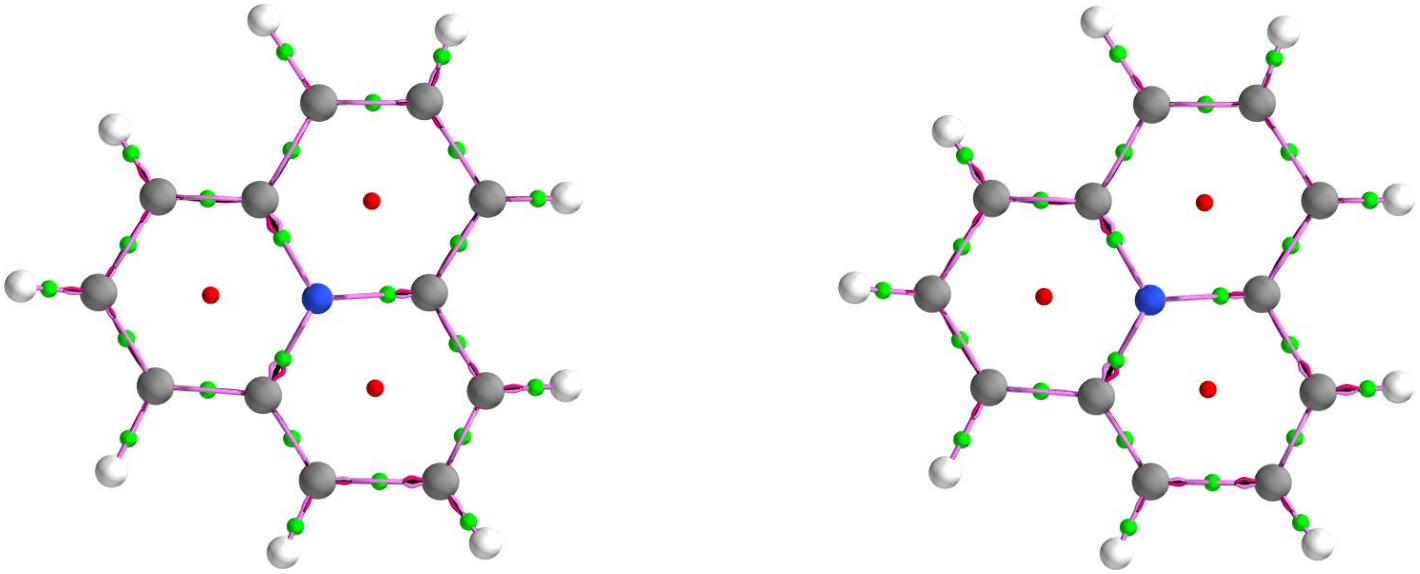

(a)

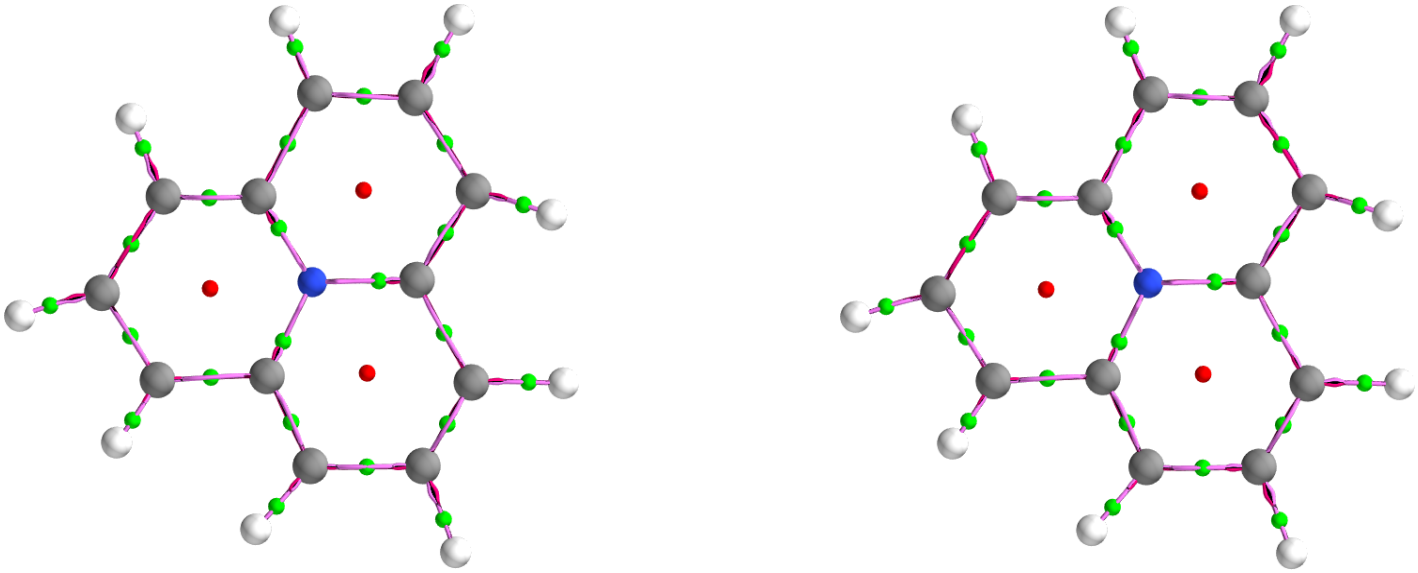

(b)

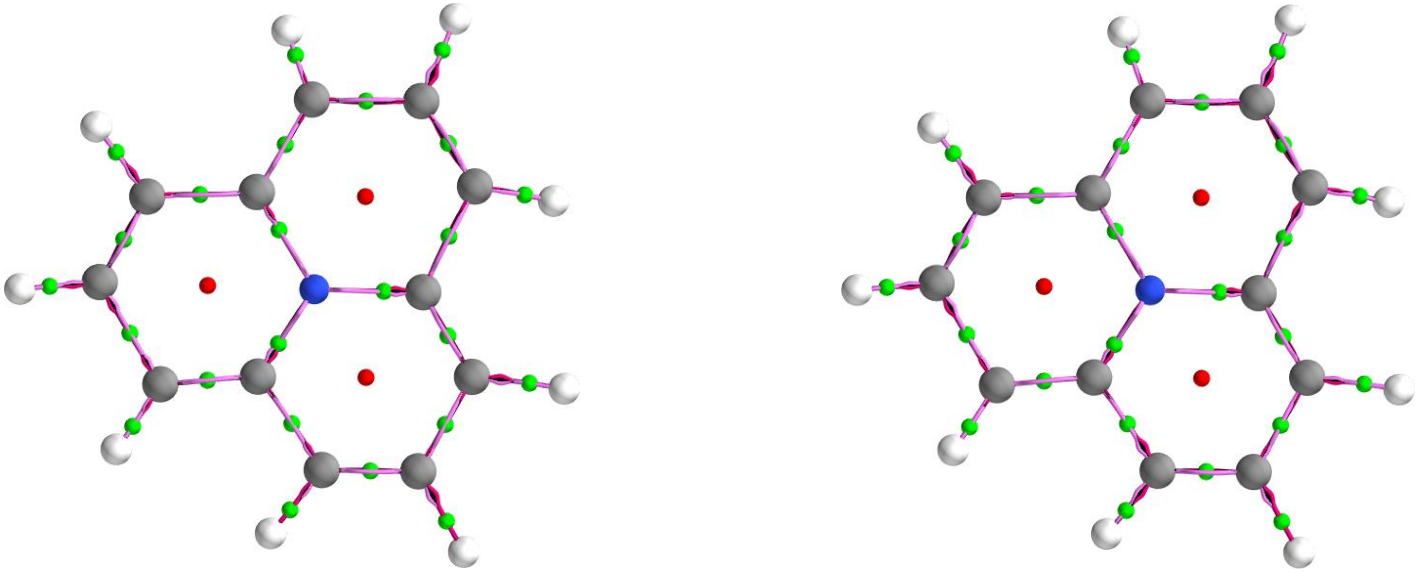

(c)

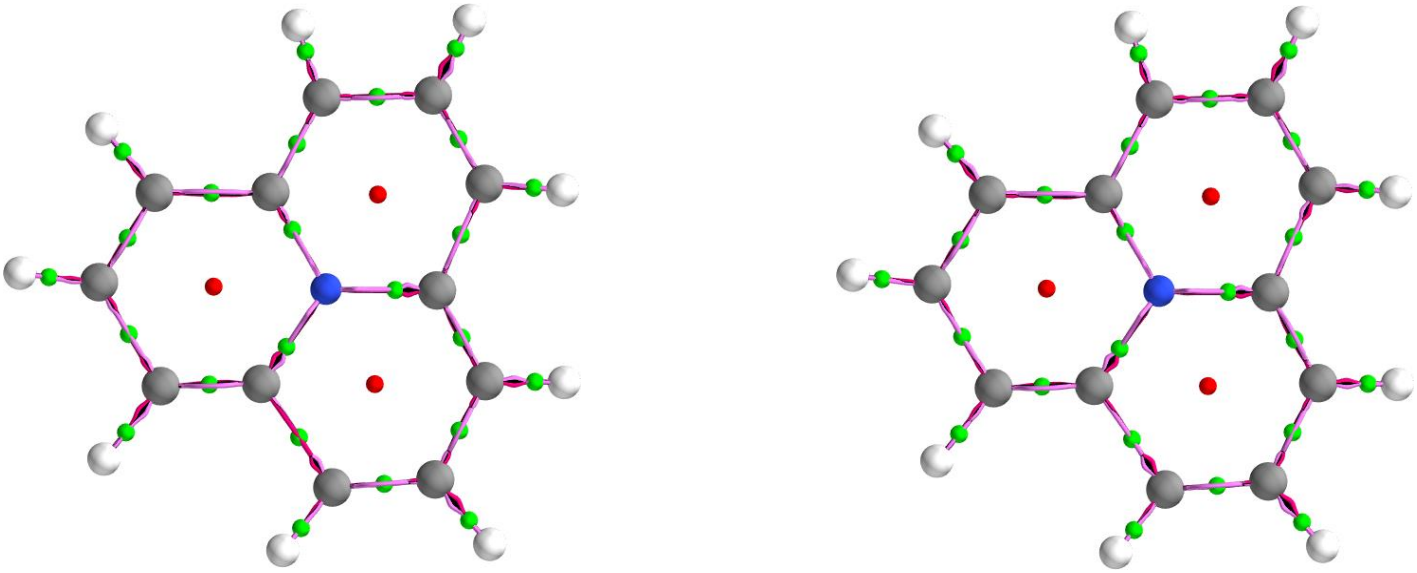

(d)

Figure S1(III). The QTAIM **{*q*,*q'*}** path-packets of the cyclazine molecular graph corresponding to the S_1 (left panel) and T_1 (right panel) states of the chirped pulse 10 fs, 45 fs, 67 fs and 90 fs with a positive energy gap $\Delta E(S_1\text{-}T_1) > 0$ are presented in each of sub-figures **(a-d)** respectively.

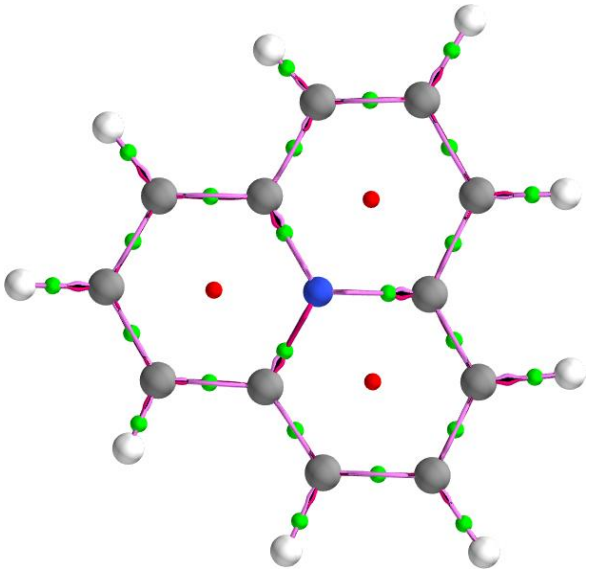
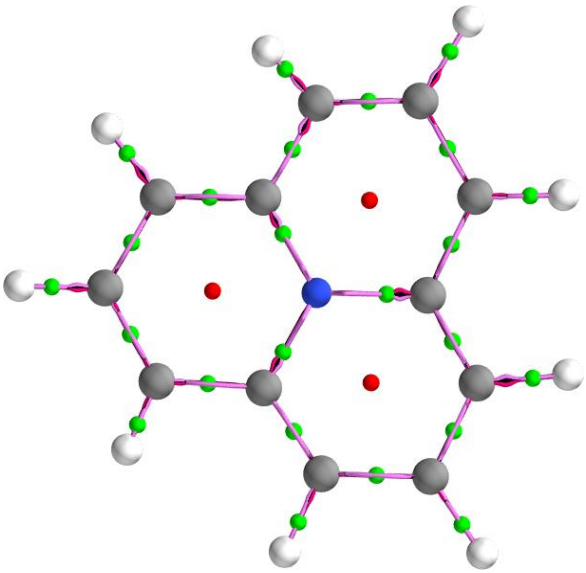

(a)

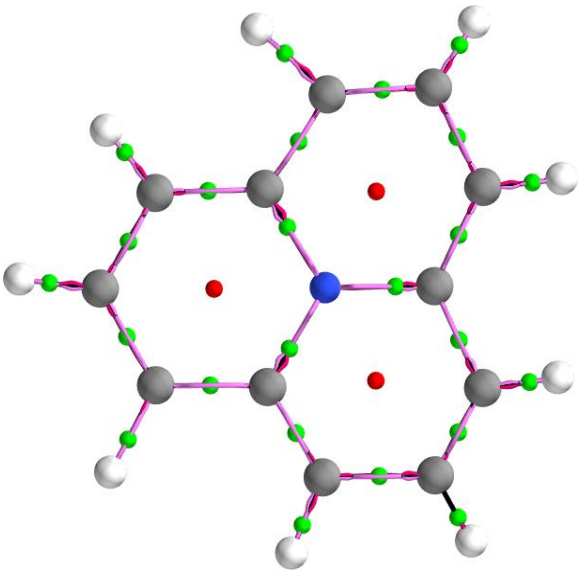
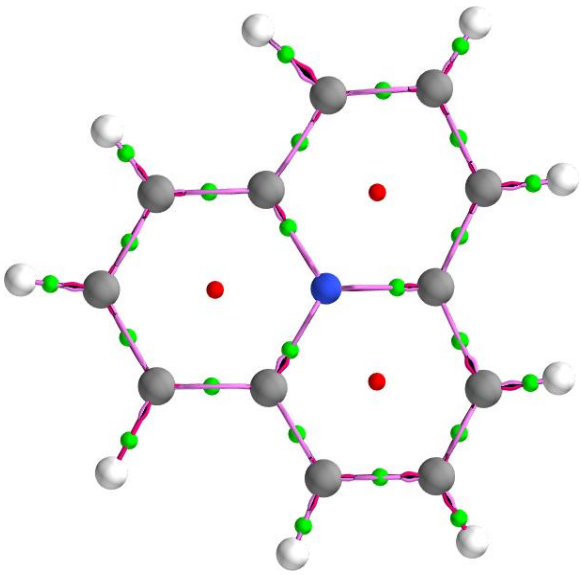

(b)

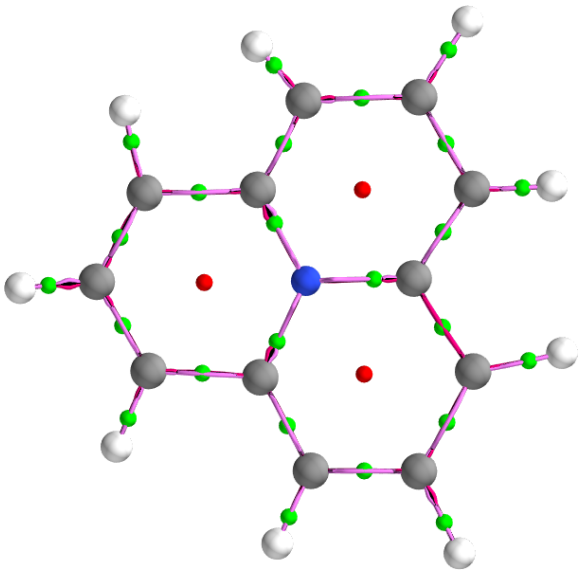
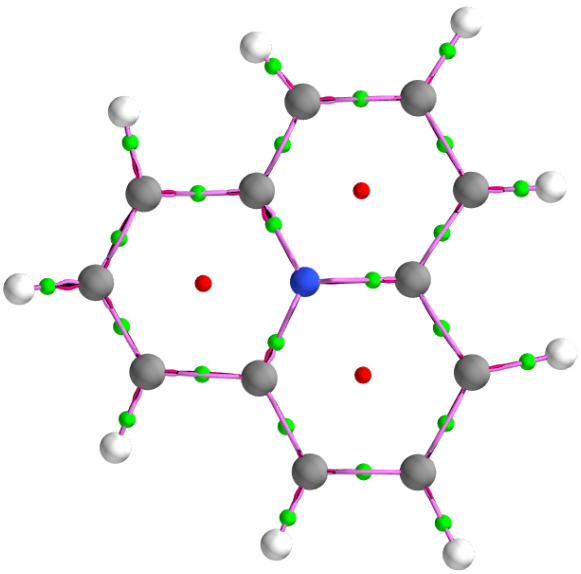

(c)

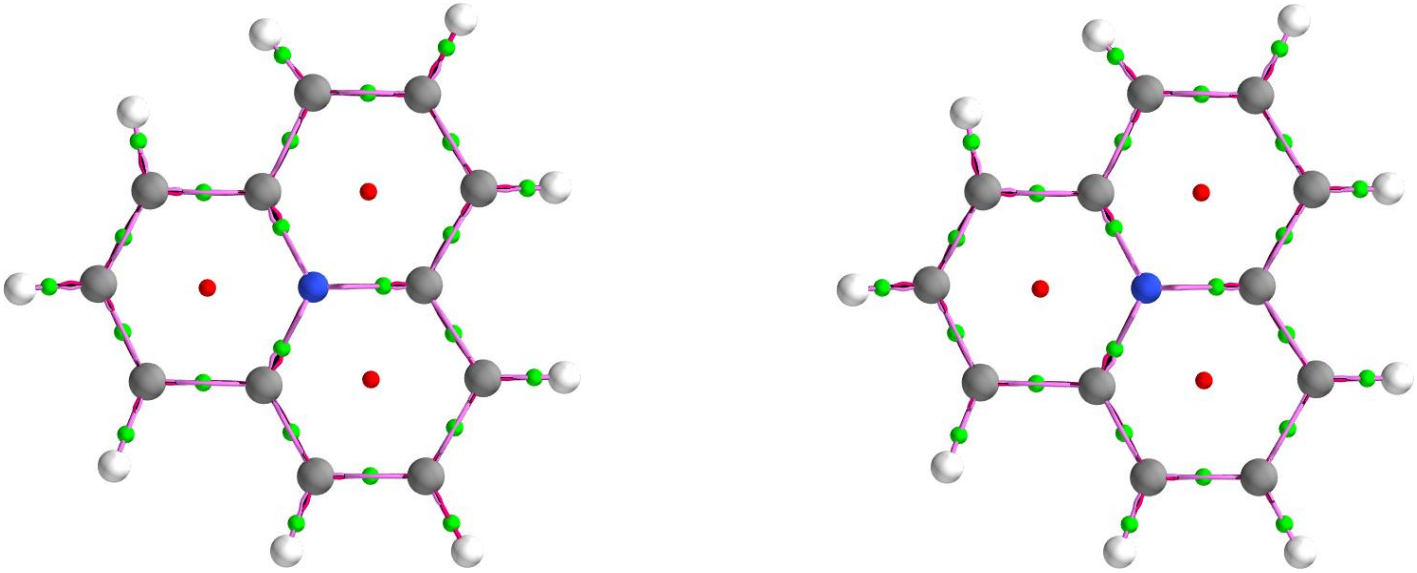

(d)

Figure S1(IV). The QTAIM ***{q,q′}*** path-packets of the cyclazine molecular graph corresponding to the S_1 (left panel) and T_1 (right panel) states of the chirped pulse 5fs, 30fs, 78fs and 100fs with a negative energy gap $\Delta E(S_1\text{-}T_1) < 0$ are presented in each of sub-figures **(a-d)** respectively.

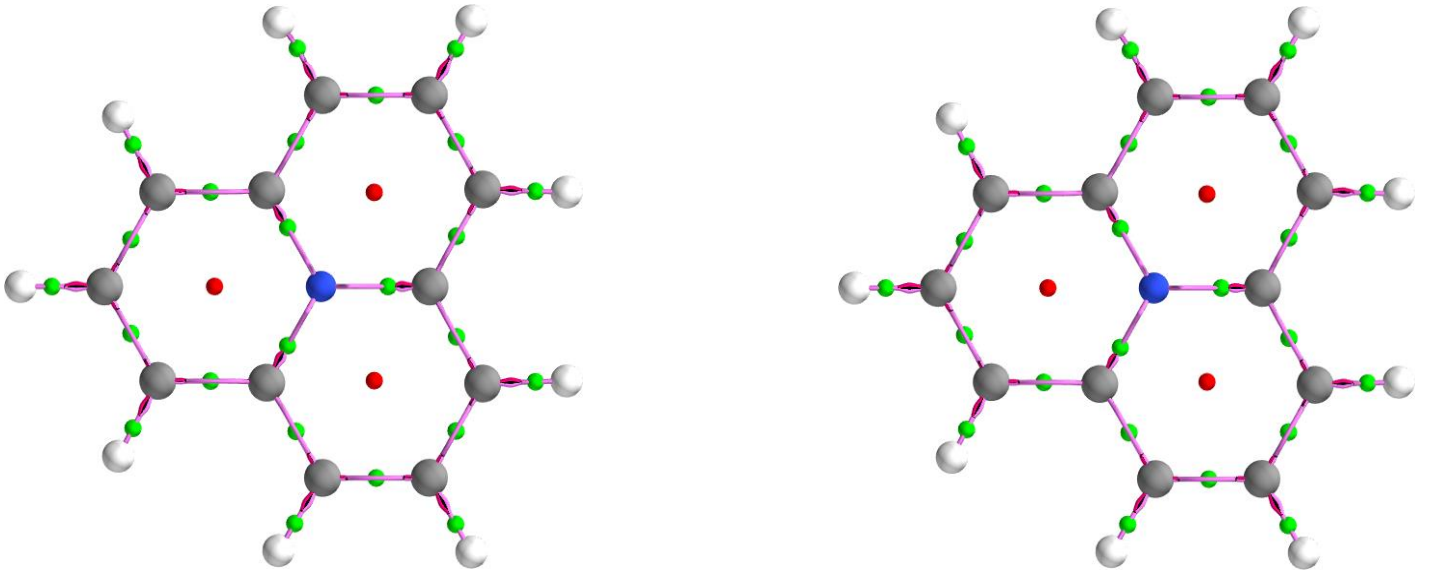

(a)

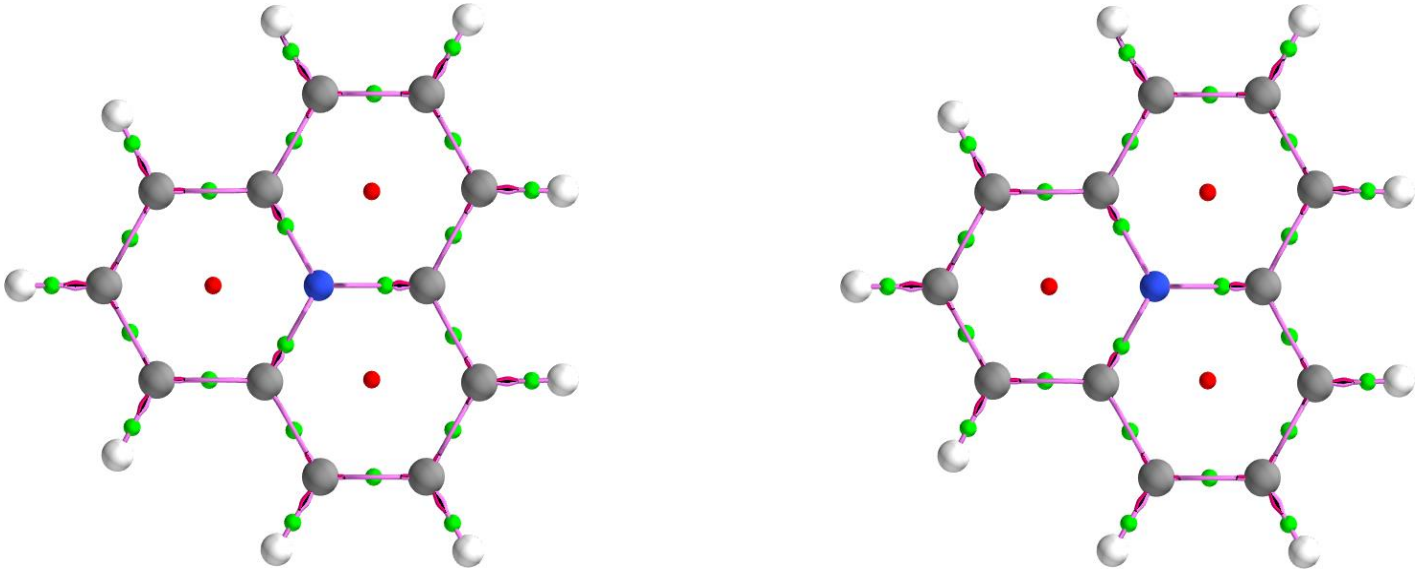

(b)

Figure S1(V). The QTAIM ***{q,q'}*** path-packets of the cyclazine molecular graph corresponding to the S_1 (left panel) and T_1 (right panel) states of an applied electric(**E**)-field = ±0.2 a.u are presented in each of sub-figures **(a-b)** respectively.

2. Supplementary Materials S2.

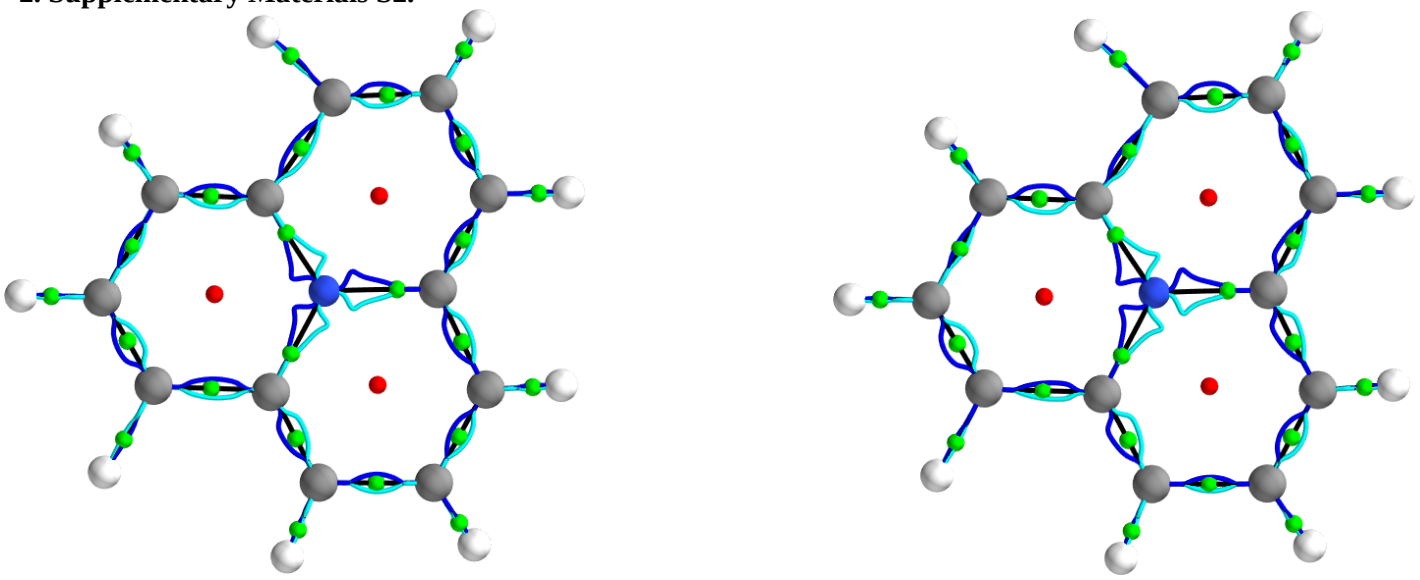

(a)

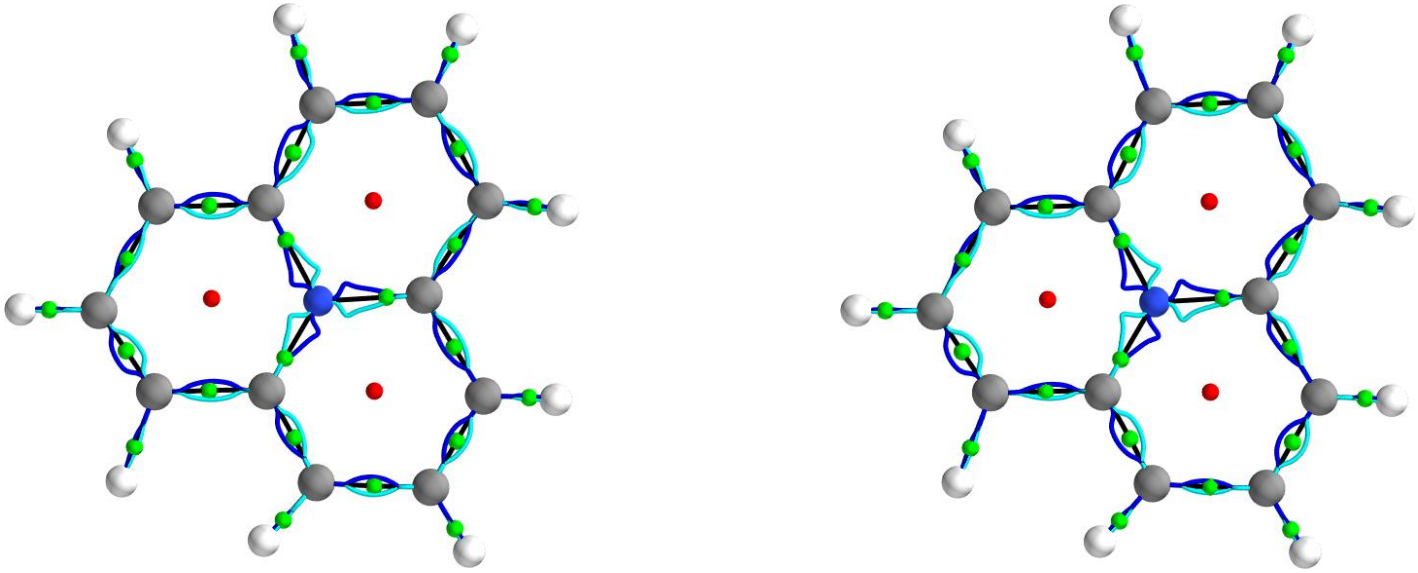

(b)

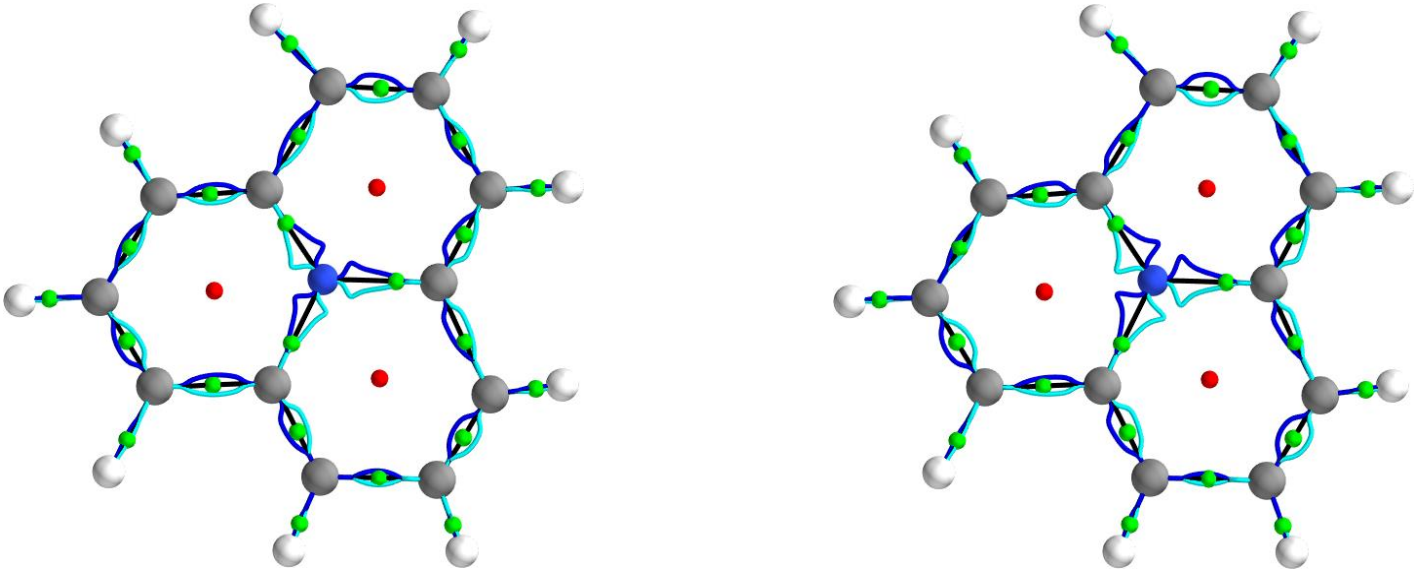

(c)

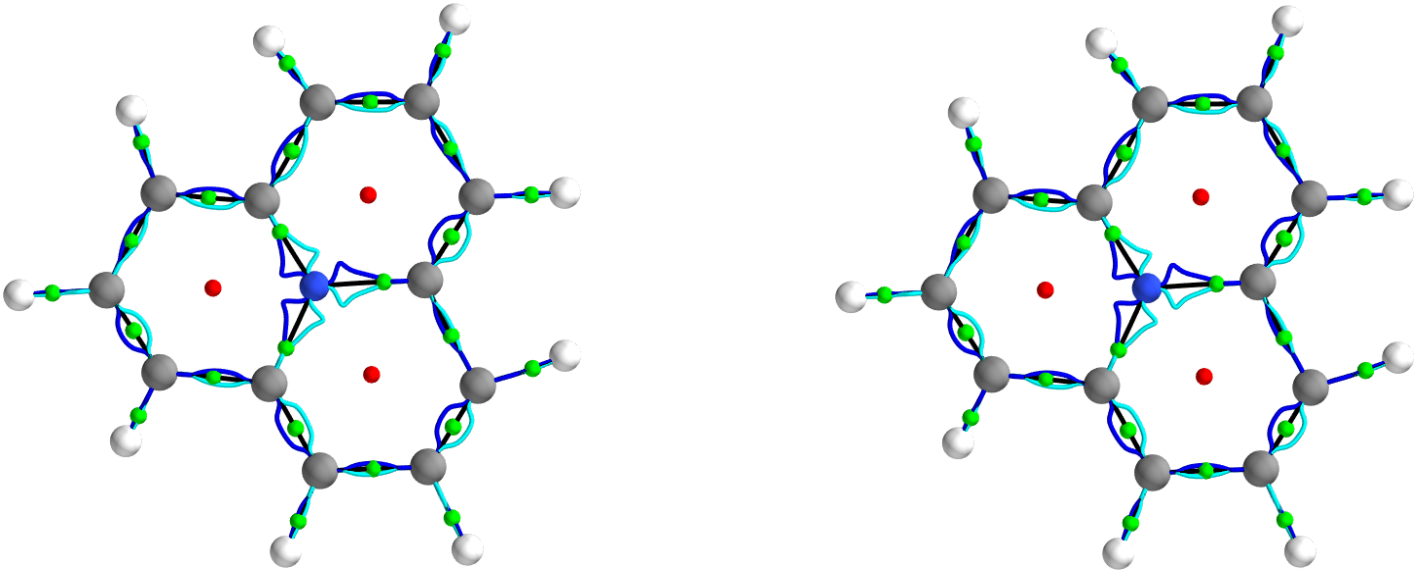

(d)

Figure S2(I). The QTAIM **{*p*,*p'*}** path-packets of the cyclazine molecular graph corresponding to the S_1 (left panel) and T_1 (right panel) states of the unchirped pulse 30 fs, 40 fs, 50 fs and 75fs with a positive energy gap $\Delta E(S_1\text{-}T_1) > 0$ are presented in each of sub-figures **(a-d)** respectively.

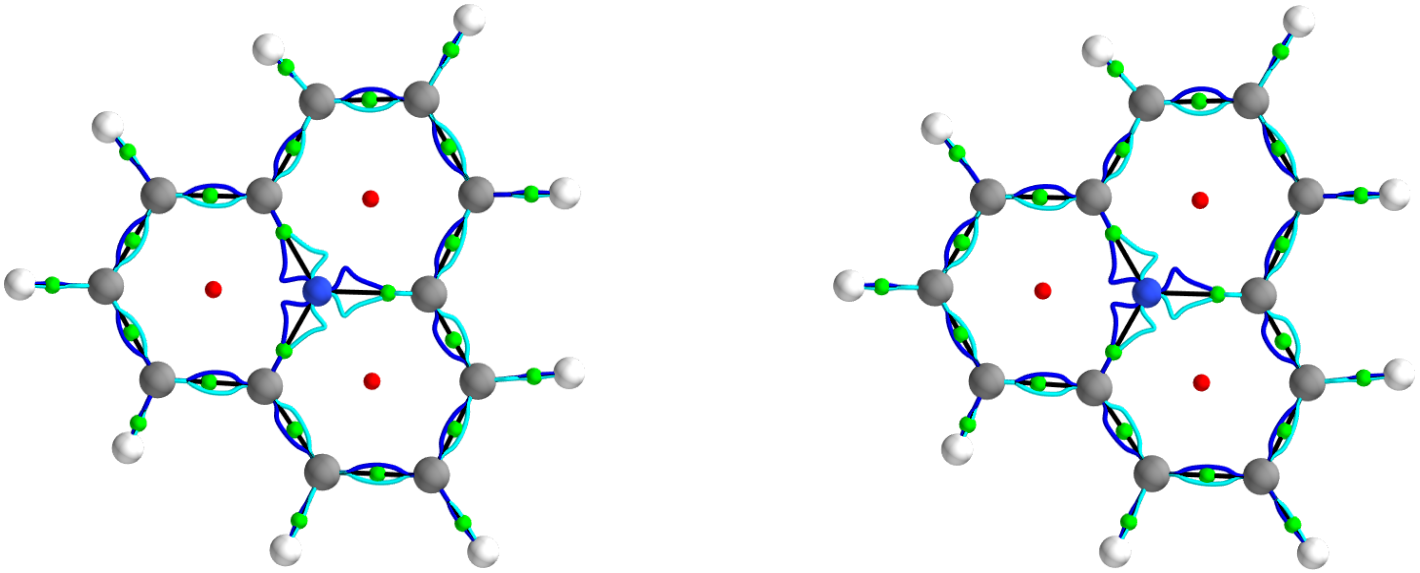

(a)

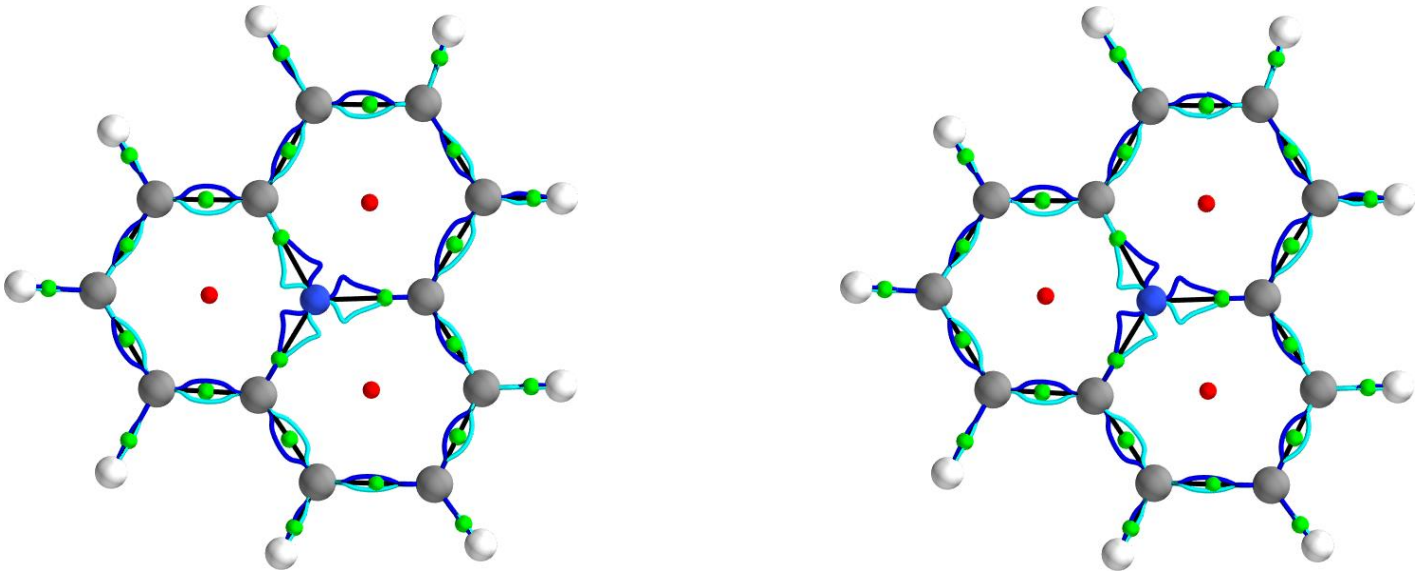

(b)

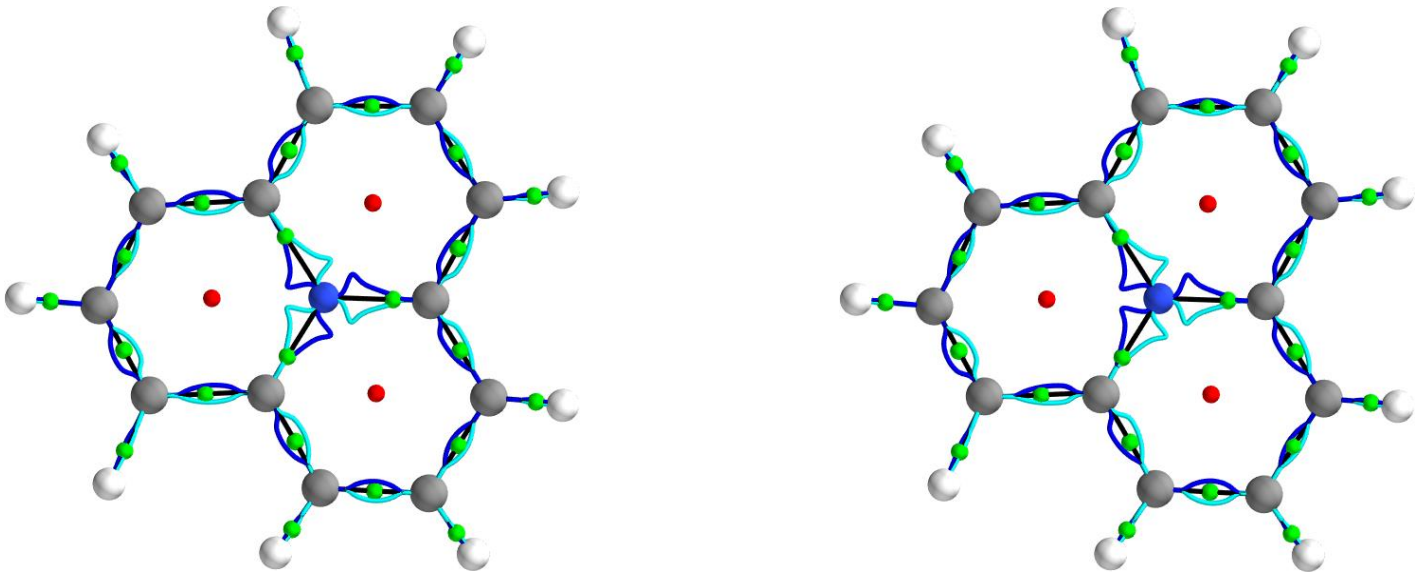

(c)

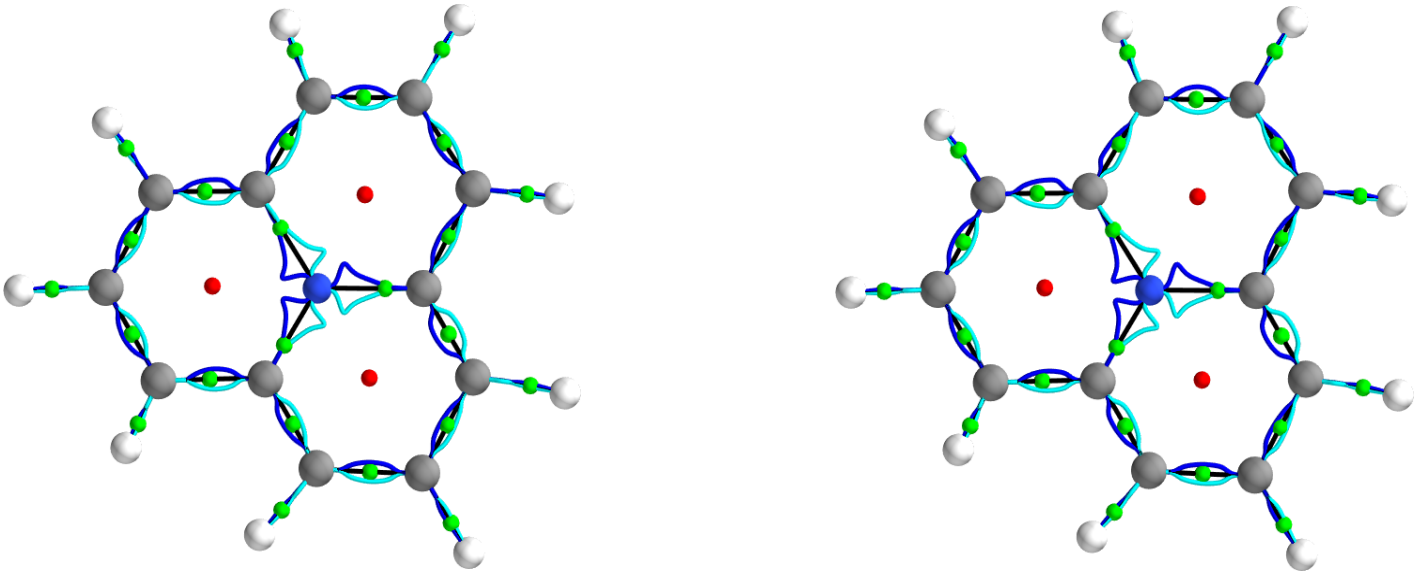

(d)

Figure S2(II). The QTAIM ***{p,p'}*** path-packets of the cyclazine molecular graph corresponding to the S_1 (left panel) and T_1 (right panel) states of the unchirped pulse 5fs, 10fs, 60fs and 65fs with a negative energy gap $\Delta E(S_1\text{-}T_1) < 0$ are presented in each of sub-figures **(a-d)** respectively.

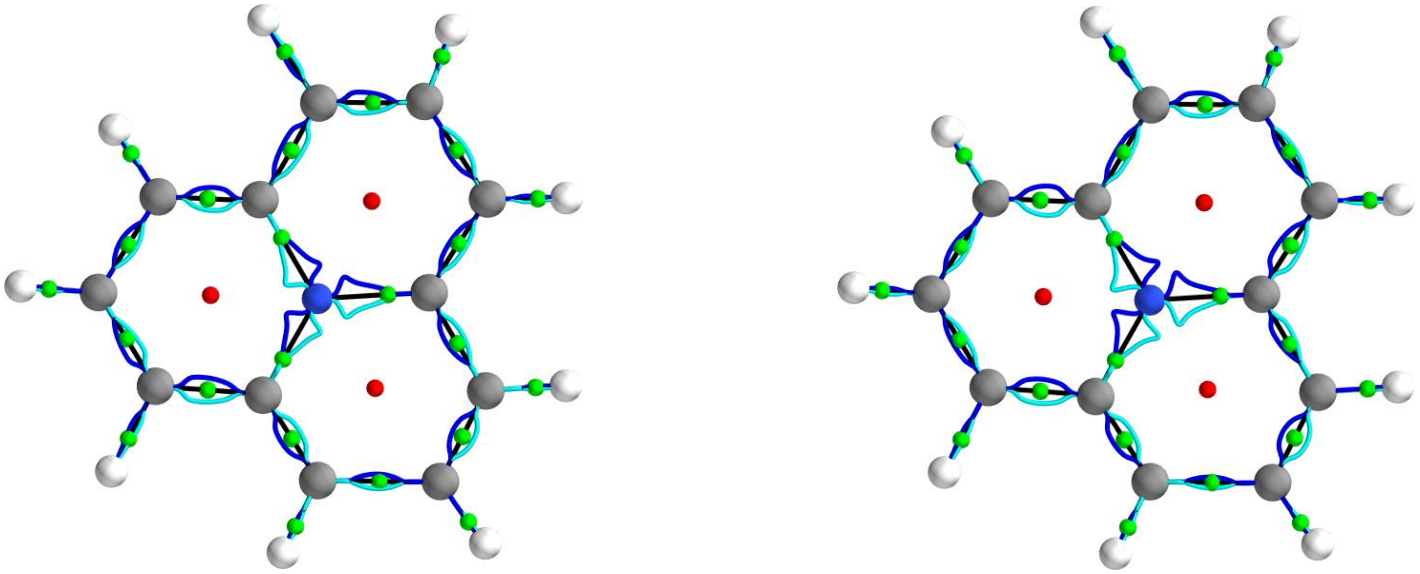

(a)

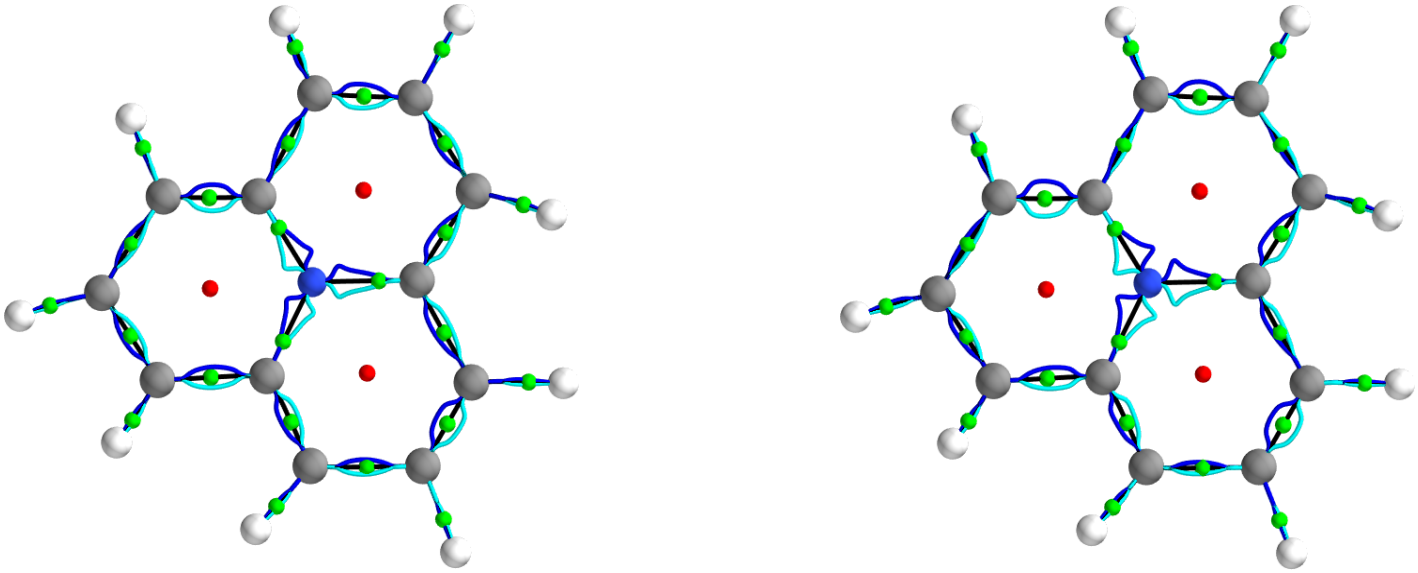

(b)

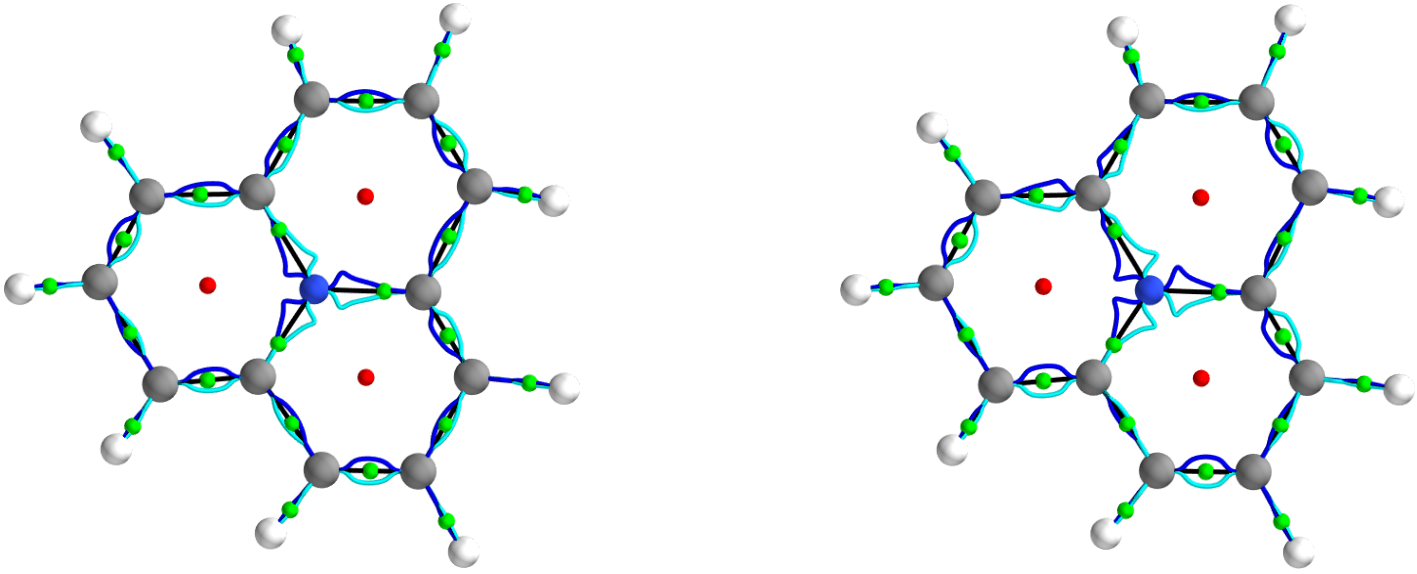

(c)

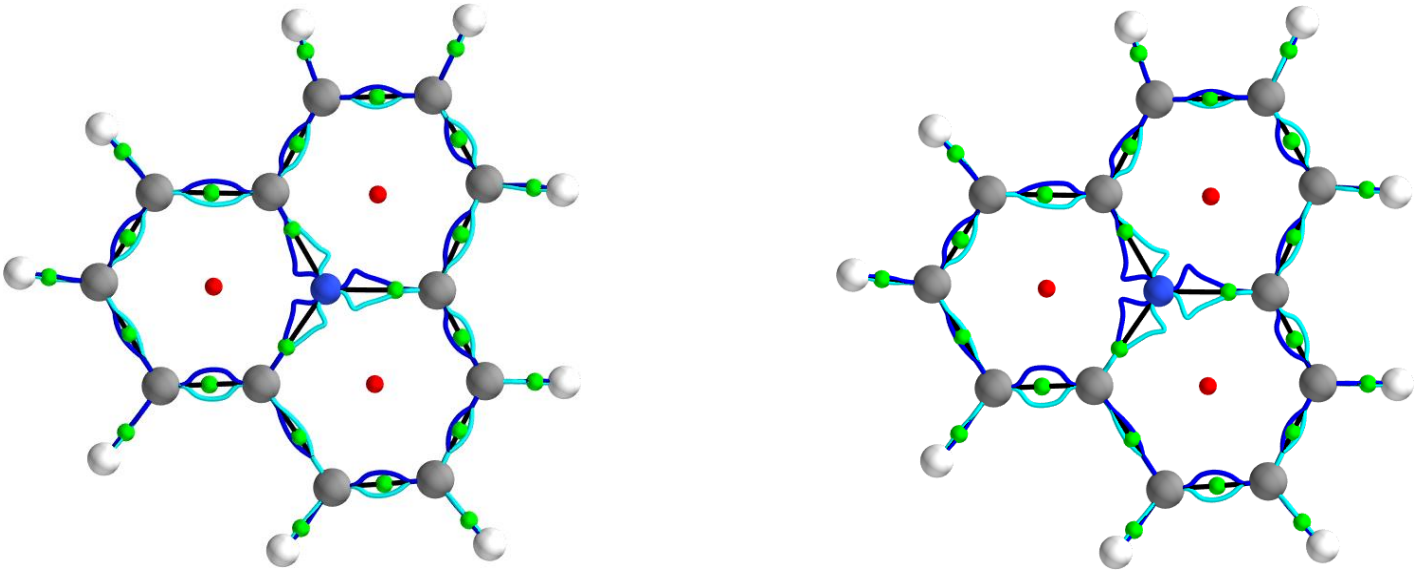

(d)

Figure S2(III). The QTAIM ***{p,p'}*** path-packets of the cyclazine molecular graph corresponding to the S_1 (left panel) and T_1 (right panel) states of the chirped pulse 10 fs, 45 fs, 67 fs and 90 fs with a positive energy gap $\Delta E(S_1\text{-}T_1) > 0$ are presented in each of sub-figures **(a-d)** respectively.

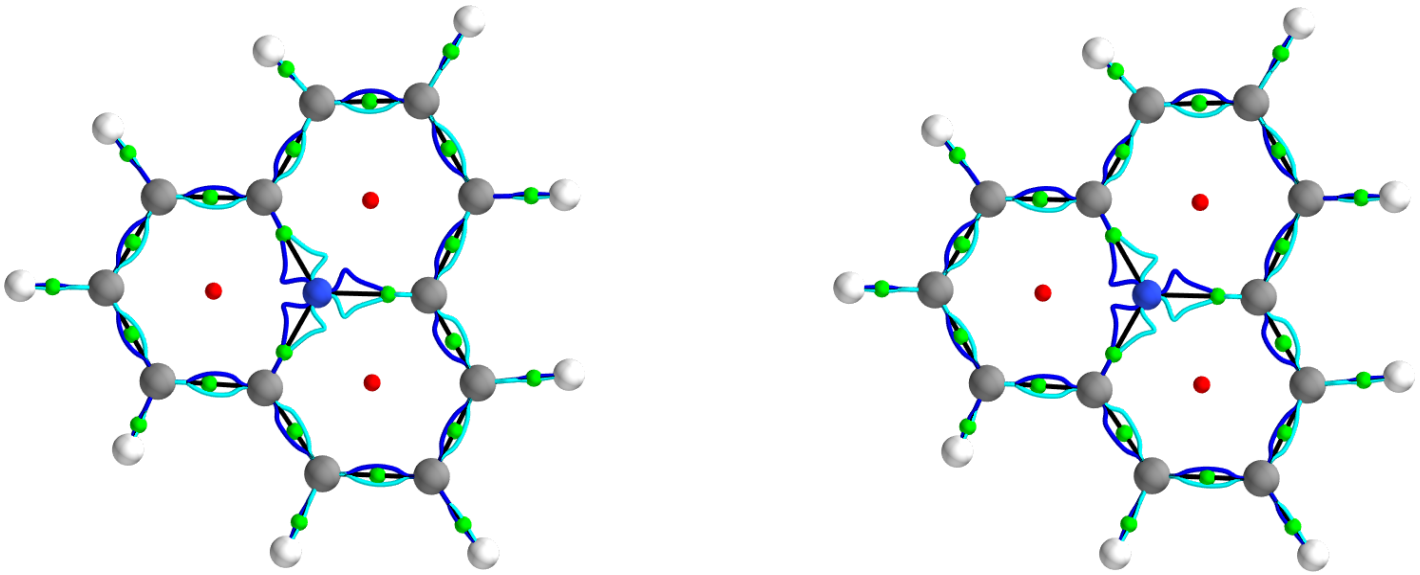

(a)

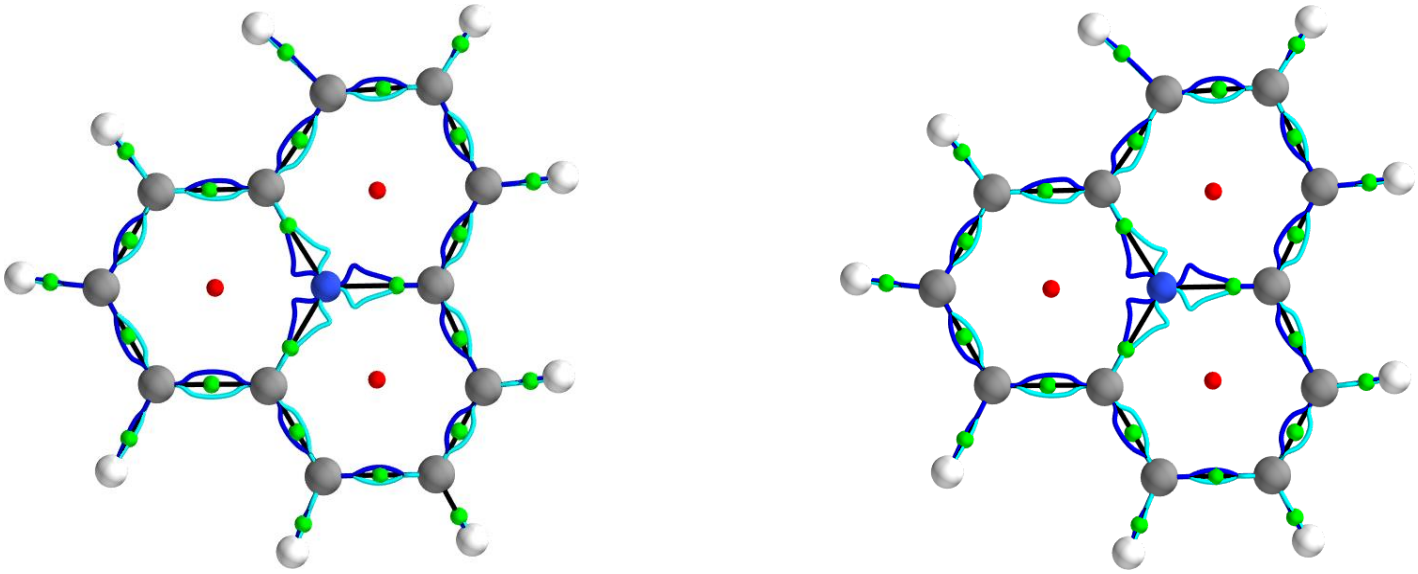

(b)

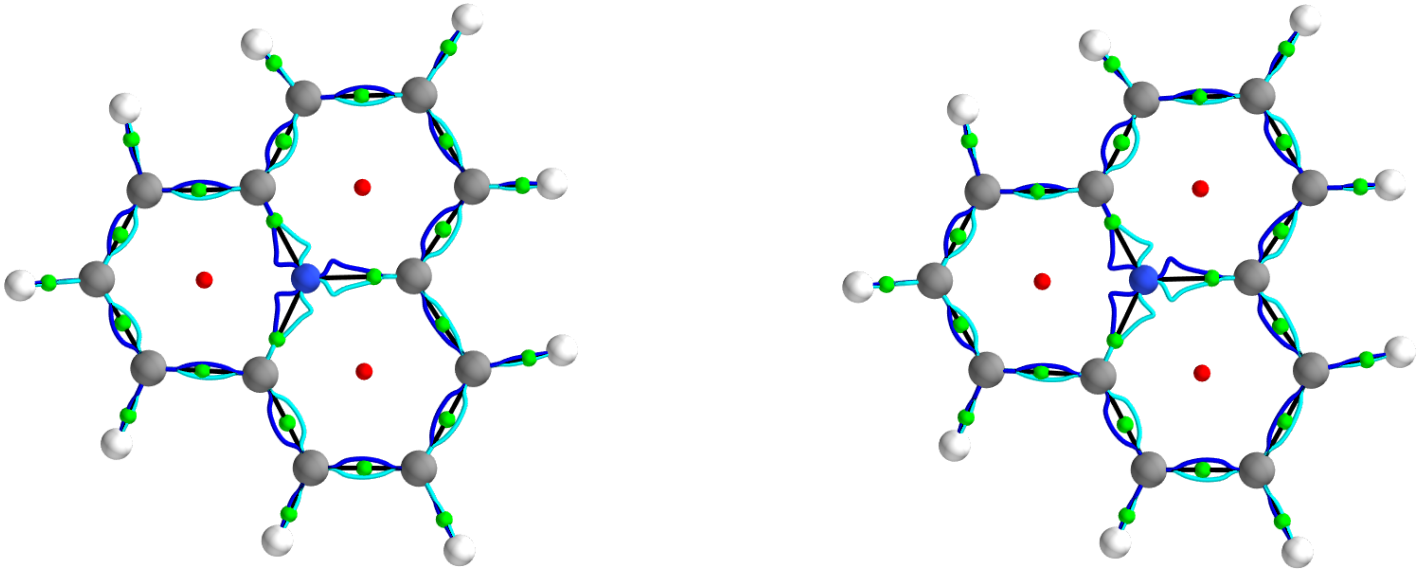

(c)

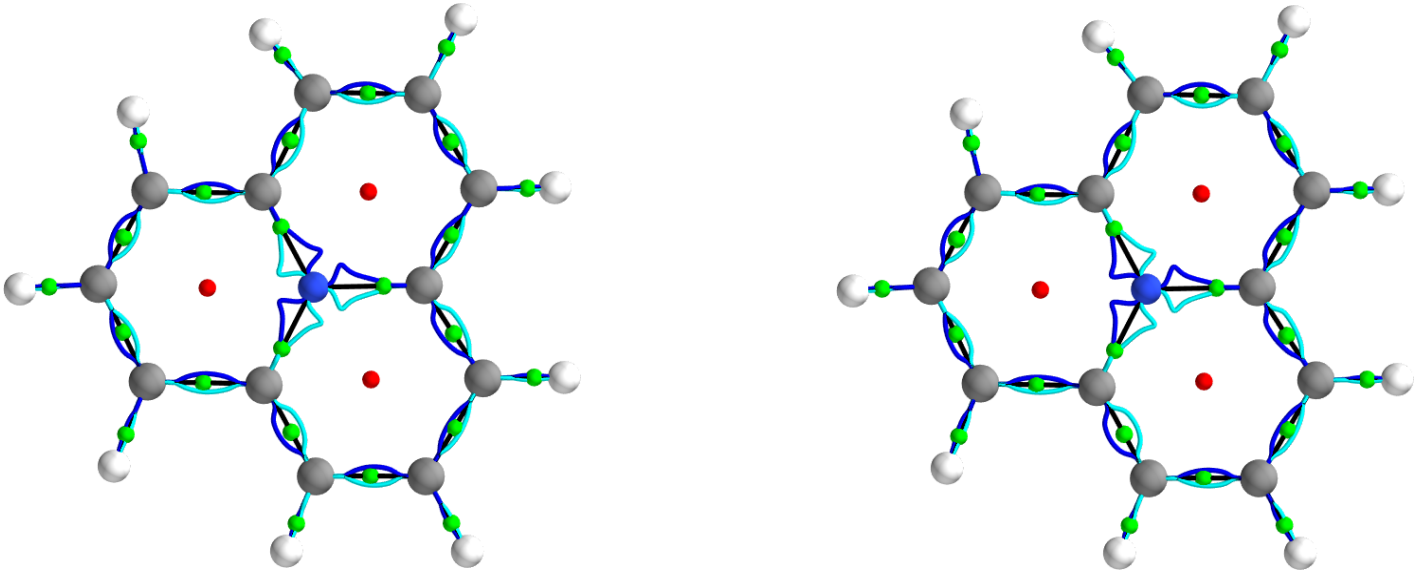

(d)

Figure S2(IV). The QTAIM ***{p,p'}*** path-packets of the cyclazine molecular graph corresponding to the S_1 (left panel) and T_1 (right panel) states of the chirped pulse 5fs, 30fs, 78fs and 100fs with a negative energy gap $\Delta E(S_1\text{-}T_1) < 0$ are presented in each of sub-figures **(a-d)** respectively.

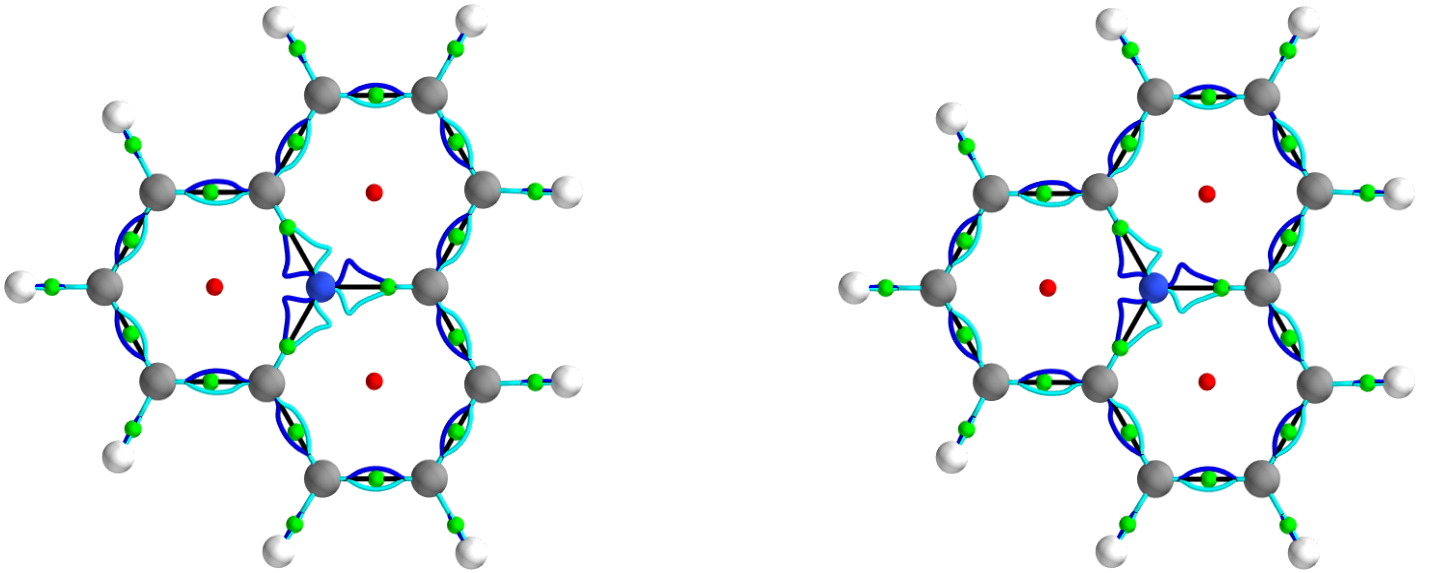

(a)

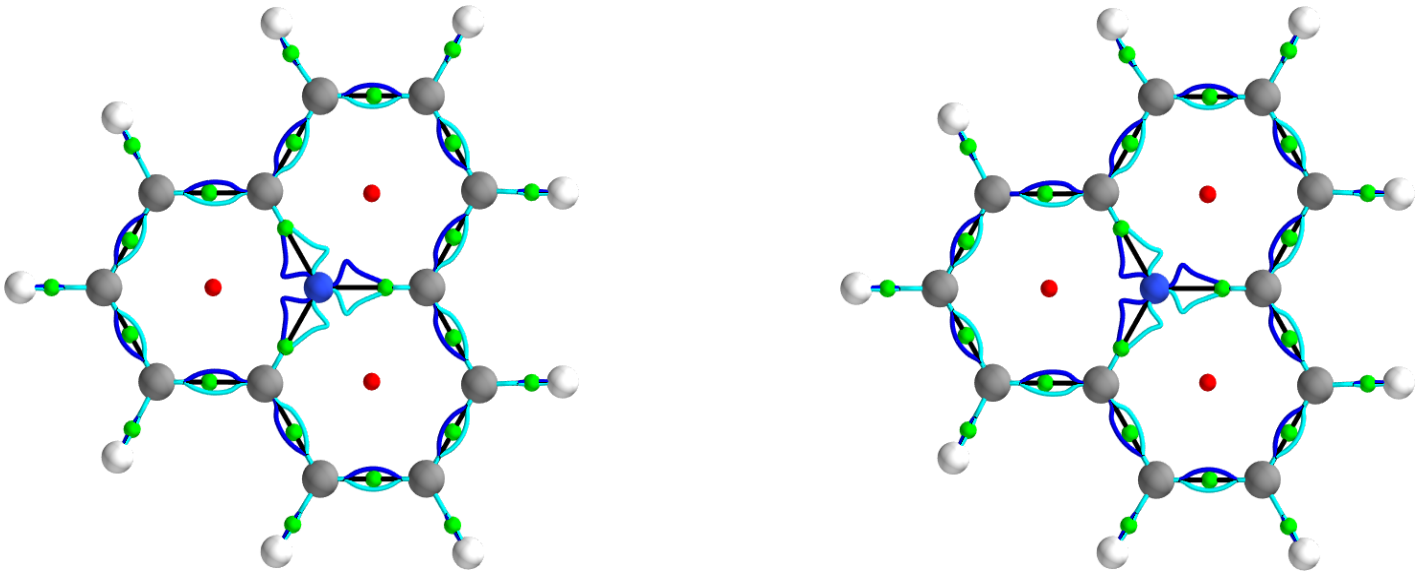

(b)

Figure S2(V). The QTAIM ***{p,p'}*** path-packets of the cyclazine molecular graph corresponding to the S_1 (left panel) and T_1 (right panel) states of an applied electric(**E**)-field = ±0.2 a.u are presented in each of sub-figures **(a-b)** respectively.

3. Supplementary Materials S3.

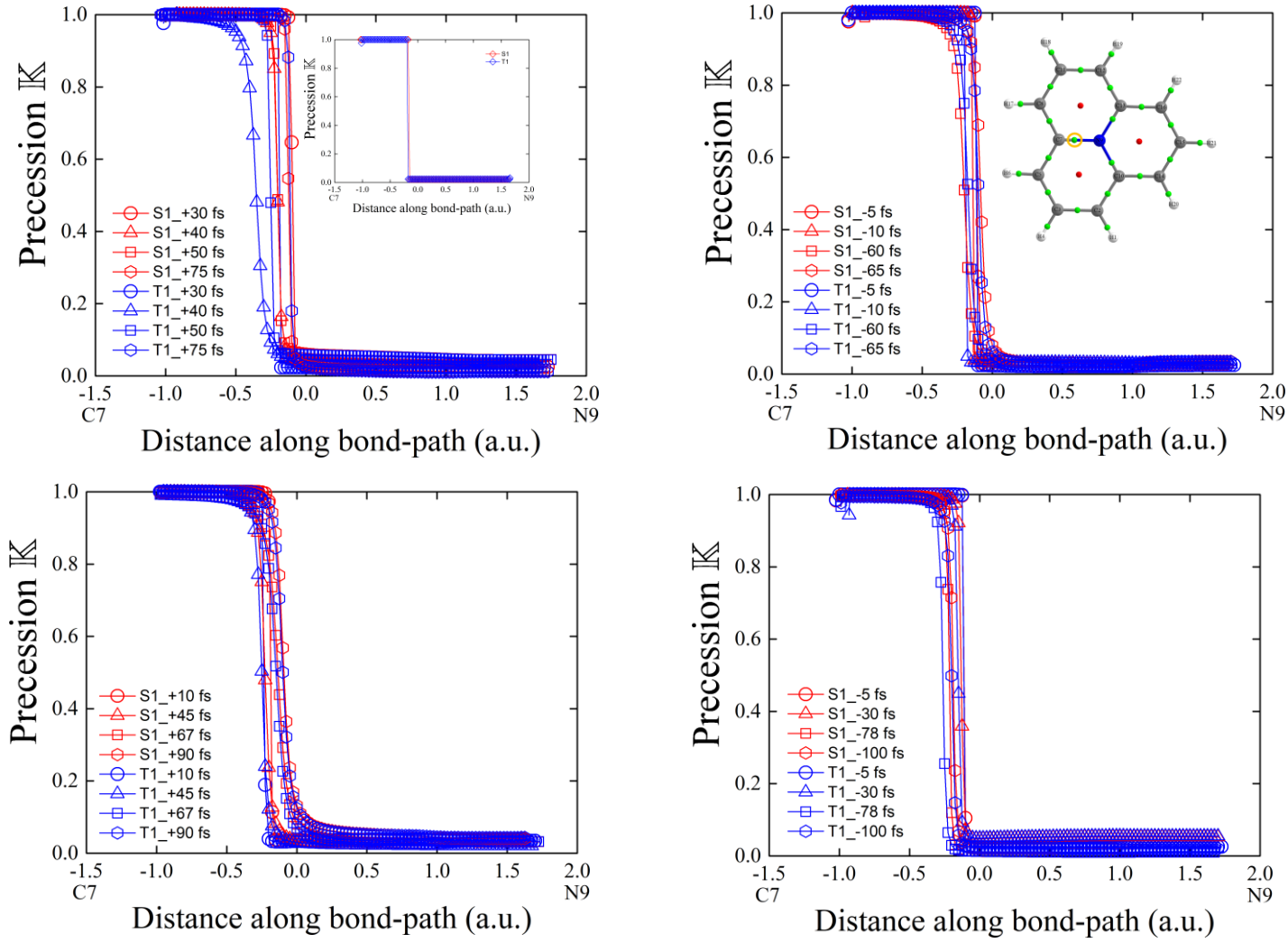

Figure S3(I). The values of the precession 𝕂 along the C7-N9 *BCP* bond-paths for the S_1 and T_1 states of the unchirped pulse with a positive energy gap $\Delta E(S_1\text{-}T_1) > 0$ (top-left) of sub-figure, the unchirped pulse with a negative energy gap $\Delta E(S_1\text{-}T_1) < 0$ (top-right) of sub-figure. The chirped pulse with $\Delta E(S_1\text{-}T_1) > 0$ (bottom-left) of sub-figure and the chirped pulses with $\Delta E(S_1\text{-}T_1) < 0$ (bottom-right) of sub-figure.

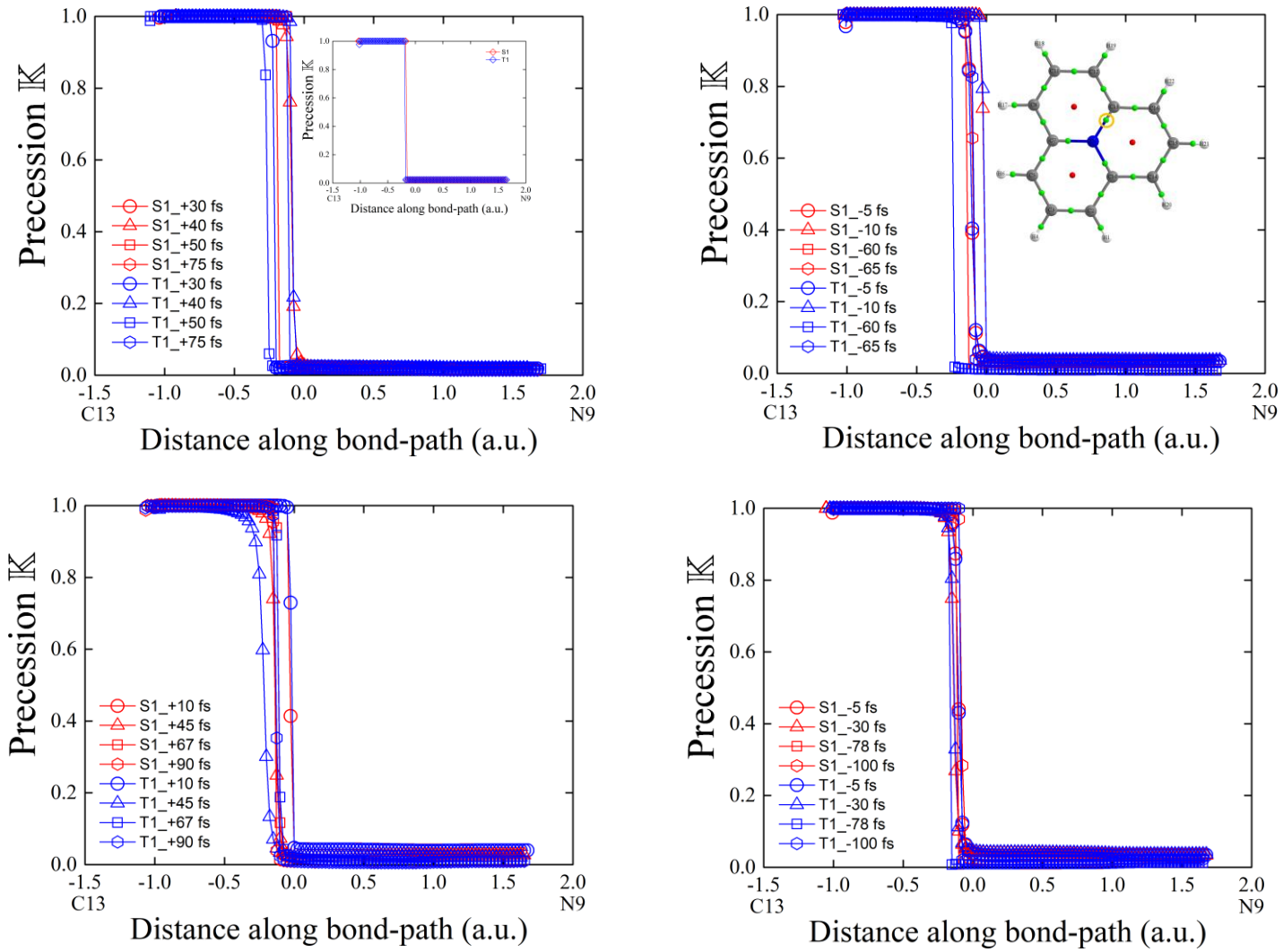

Figure S3(II). The values of the precession 𝕂 along the C13-N9 *BCP* bond-paths for the S_1 and T_1 states of the unchirped pulse with a positive energy gap $\Delta E(S_1\text{-}T_1) > 0$ (top-left) of sub-figure, the unchirped pulse with a negative energy gap $\Delta E(S_1\text{-}T_1) < 0$ (top-right) of sub-figure. The chirped pulse with $\Delta E(S_1\text{-}T_1) > 0$ (bottom-left) of sub-figure and the chirped pulses with $\Delta E(S_1\text{-}T_1) < 0$ (bottom-right) of sub-figure.

The profiles of the $\mathbb{K}$ for the C10-C2 *BCP* with the unchirped laser pulse corresponding to a S_1 state at a given time with $\Delta E(S_1\text{-}T_1) > 0$ responding less than the corresponding T_1 state the same time, see the top-left panel of **Figure S3(III)**. The corresponding $\mathbb{K}$ for the C10-C2 *BCP* with $\Delta E(S_1\text{-}T_1) < 0$ and unchirped pulse result in a mixing of the $\mathbb{K}$ profiles of the S_1 and T_1 states, see the top-right panel of **Figure S3(III)**. The effect of the chirped laser pulse on the $\mathbb{K}$ profiles with a positive energy gap $\Delta E(S_1\text{-}T_1) > 0$ is to spread out the $\mathbb{K}$ profiles of the S_1 and T_1 states, see the bottom-left panel of **Figure S3(III)**. Conversely, the effect of the chirped pulse on negative energy gap $\Delta E(S_1\text{-}T_1) < 0$ is to contract the $\mathbb{K}$ profiles corresponding to the S_1 and T_1 states to closer together, see the bottom-right panel of **Figure S3(III)**.

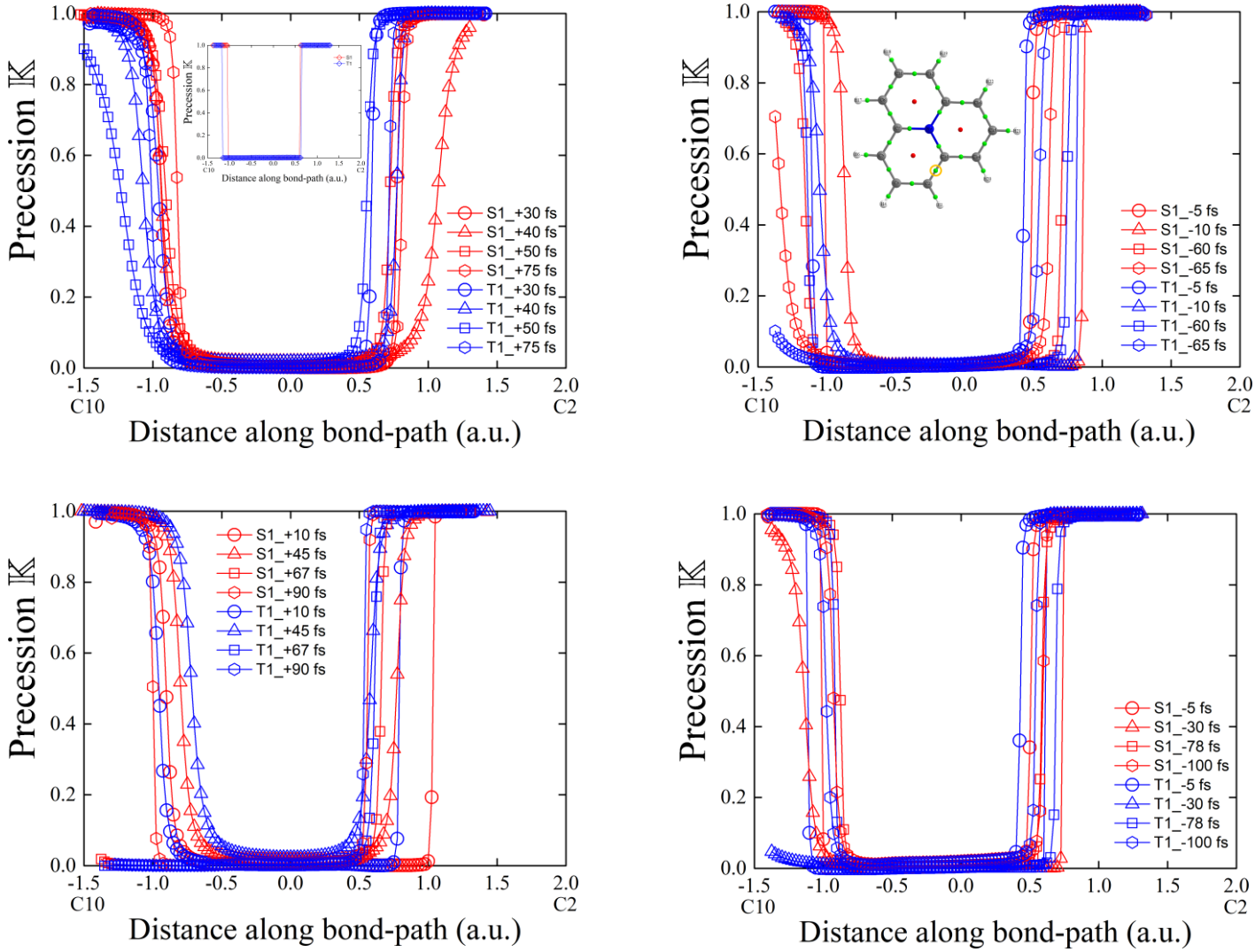

Figure S3(III). The values of the precession $\mathbb{K}$ along the C10-C2 *BCP* bond-paths for the S_1 and T_1 states of the unchirped pulse with a positive energy gap $\Delta E(S_1\text{-}T_1) > 0$ (top-left) of sub-figure, the unchirped pulse with a negative energy gap $\Delta E(S_1\text{-}T_1) < 0$ (top-right) of sub-figure. The chirped pulse with $\Delta E(S_1\text{-}T_1) > 0$ (bottom-left) of sub-figure and the chirped pulse s with $\Delta E(S_1\text{-}T_1) < 0$ (bottom-right) of sub-figure.

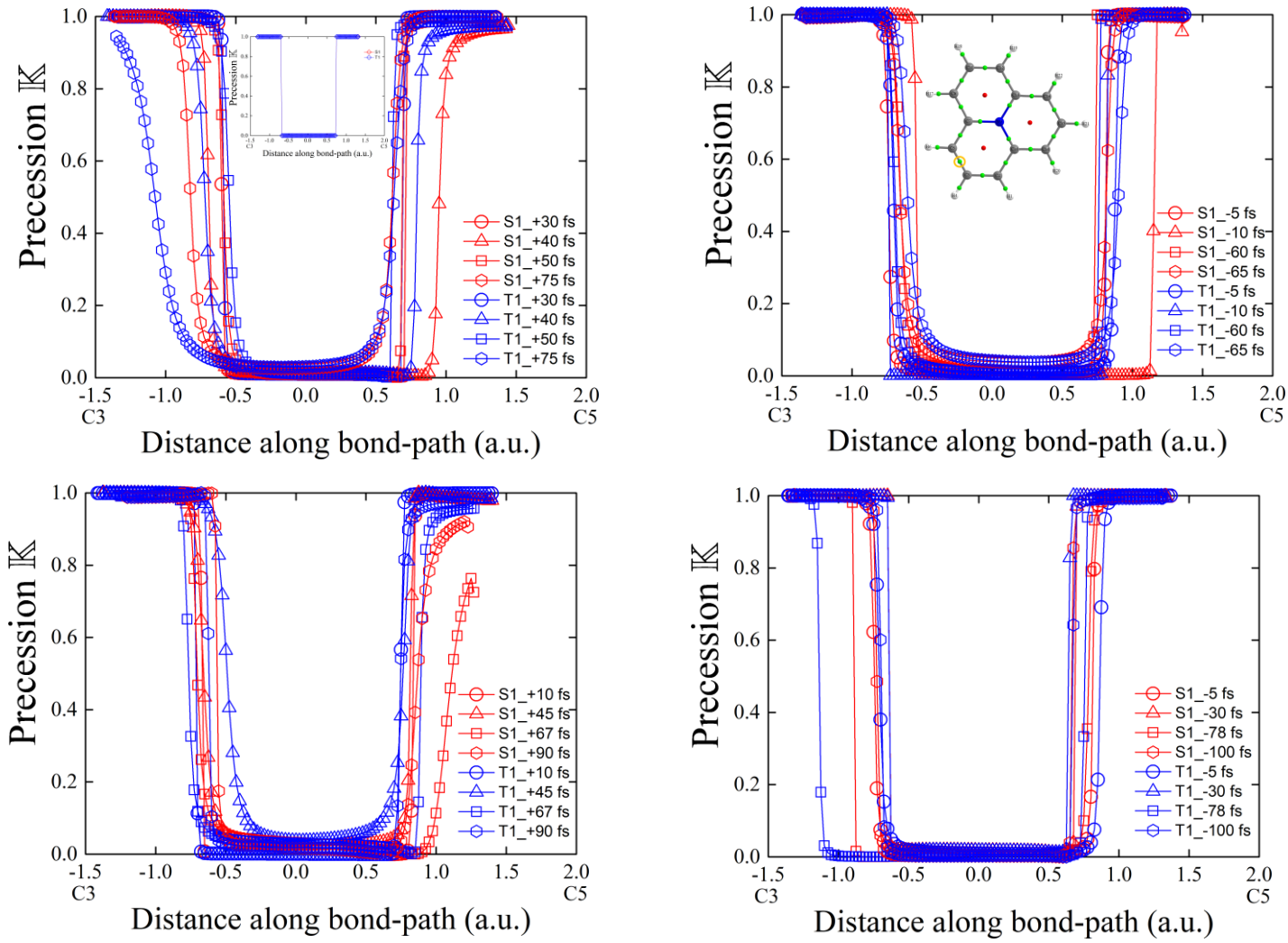

Figure S3(IV). The values of the precession 𝕂 along the C3-C5 *BCP* bond-paths for the S_1 and T_1 states of the unchirped pulse with a positive energy gap $\Delta E(S_1\text{-}T_1) > 0$ (top-left) of sub-figure, the unchirped pulse with a negative energy gap $\Delta E(S_1\text{-}T_1) < 0$ (top-right) of sub-figure. The chirped pulse with $\Delta E(S_1\text{-}T_1) > 0$ (bottom-left) of sub-figure and the chirped pulse s with $\Delta E(S_1\text{-}T_1) < 0$ (bottom-right) of sub-figure.

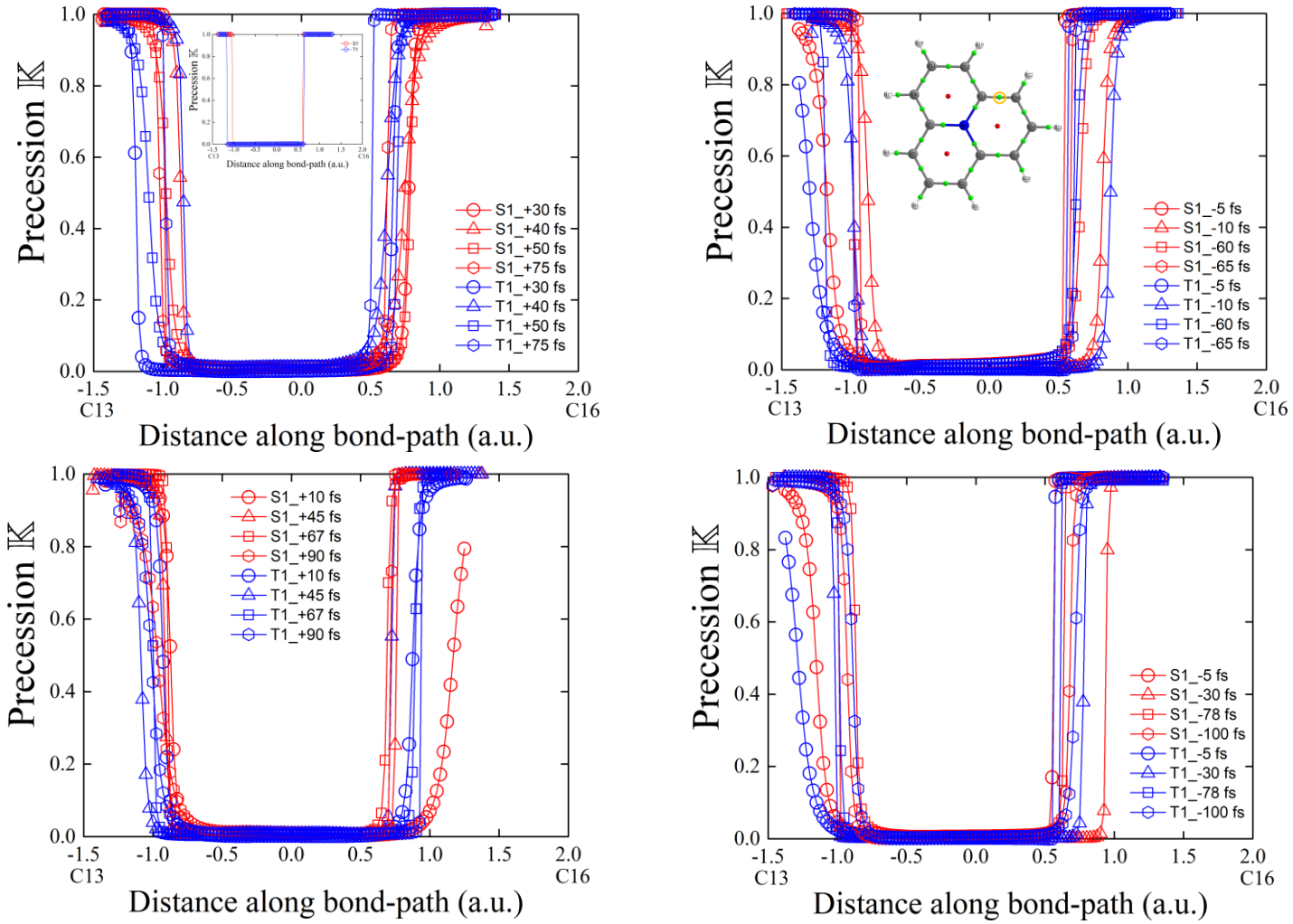

Figure S3(V). The values of the precession 𝕂 along the C13-C16 *BCP* bond-paths for the S_1 and T_1 states of the unchirped pulse with a positive energy gap $\Delta E(S_1\text{-}T_1) > 0$ (top-left) of sub-figure, the unchirped pulse with a negative energy gap $\Delta E(S_1\text{-}T_1) < 0$ (top-right) of sub-figure. The chirped pulse with $\Delta E(S_1\text{-}T_1) > 0$ (bottom-left) of sub-figure and the chirped pulse s with $\Delta E(S_1\text{-}T_1) < 0$ (bottom-right) of sub-figure.